Published online 13 July 2009

Nucleic Acids Research, 2009, Vol. 37, No. 16 ***5511–5528***
doi:10.1093/nar/gkp571

The role of deadenylation in the degradation of unstable mRNAs in trypanosomes

Angela Schwede, Theresa Manful, Bhaskar Anand Jha, Claudia Helbig, Natalia Bercovich, Mhairi Stewart and Christine Clayton*

Zentrum für Molekulare Biologie (ZMBH), DKFZ-ZMBH Alliance, Im Neuenheimer Feld 282, D-69120 Heidelberg, Germany

Received May 15, 2009; Revised June 16, 2009; Accepted June 20, 2009

ABSTRACT

Removal of the poly(A) tail is the first step in the degradation of many eukaryotic mRNAs. In metazoans and yeast, the Ccr4/Caf1/Not complex has the predominant deadenylase activity, while the Pan2/Pan3 complex may trim poly(A) tails to the correct size, or initiate deadenylation. In trypanosomes, turnover of several constitutively-expressed or long-lived mRNAs is not affected by depletion of the 5′–3′ exoribonuclease XRNA, but is almost completely inhibited by depletion of the deadenylase CAF1. In contrast, two highly unstable mRNAs, encoding EP procyclin and a phosphoglycerate kinase, PGKB, accumulate when XRNA levels are reduced. We here show that degradation of *EP* mRNA was partially inhibited after CAF1 depletion. RNAi-targeting trypanosome PAN2 had a mild effect on global deadenylation, and on degradation of a few mRNAs including *EP*. By amplifying and sequencing degradation intermediates, we demonstrated that a reduction in XRNA had no effect on degradation of a stable mRNA encoding a ribosomal protein, but caused accumulation of *EP* mRNA fragments that had lost substantial portions of the 5′ and 3′ ends. The results support a model in which trypanosome mRNAs can be degraded by at least two different, partially independent, cytoplasmic degradation pathways attacking both ends of the mRNA.

INTRODUCTION

Messenger RNA degradation is an important component of the control of gene expression in eukaryotes. Messenger RNAs are generally protected from degradation by the interaction of poly(A)-binding protein (PABP) with both the poly(A) tail at the 3′-end, and the cap-binding complex at the 5′-end (1). In the simplest model, mRNA degradation is initiated by digestion of the poly(A) tail; once the tail has been shortened below a certain threshold length, poly(A)-binding protein drops off, the interaction with the 5′-end is disrupted and the RNA ends become available for digestion (2,3). Three major deadenylases are known: PARN, Pan2/Pan3 and the Ccr4/Caf1/Not complex.

The poly(A) ribonuclease PARN has specialized functions, such as deadenylation of stored mRNAs during the maturation of oocytes (4,5) and regulation of embryogenesis in plants (6). It is stimulated by PABP (7) and by binding to the 5′ cap (5).

The Ccr4/Caf1/Not complex has the major deadenylation activity in animal cells and yeast. (8,9). In some organisms, including yeast and mammals, it contains two catalytic subunits, Ccr4 and Caf1. Ccr4 is bound to Caf1, which in turn interacts with the scaffold protein Not1. Several other subunits, with stimulatory or other functions, are also associated with Not1 (10–12). Although Ccr4 is the most active deadenylase in the *Saccharomyces cerevisiae* Ccr4/Caf1/Not complex (13), Caf1 is more important in animal cells (8,14–16). Indeed, whereas Caf1 is conserved throughout eukaryotic evolution, Ccr4 is absent in many species. In some mammalian *in vitro* extracts, degradation of an mRNA substrate is stimulated by addition of poly(A) oligoribonucleotides, suggesting that the major deadenylation activity is inhibited by PABP (3,17). This would correlate with the known inhibition of Ccr4/Caf1/Not by PABP (18).

Pan2 is the catalytic subunit of the Pan2/Pan3 deadenylase and is a member of the DEDDh subfamily of exonuclease III enzymes. In contrast with Caf1, the activity of the complex is stimulated by PABP *in vitro* (19,20).

*To whom correspondence should be addressed. Tel: 49 6221 546 876; Fax: 49 6221 545 894; Email: cclayton@zmbh.uni-heidelberg.de
Present addresses:
Natalia Bercovich, Instituto de Investigaciones en Ingeniería Genética y Biología Molecular (INGEBI), FCEyN, Dto. FBMC, Universidad de Buenos Aires, Vuelta de Obligado 2490 2P, 1428, Buenos Aires, Argentina.
Mhairi Stewart, Glasgow Biomedical Research Centre, University of Glasgow, G12 8QQ, UK.

Pan3 has stimulatory function: the C-terminal part interacts with Pan2, while the N-terminus interacts with PABP (20,21). Pan3 also has a central kinase domain, the role of which is unknown. Pan2/3 is found in the yeast nucleus and cytoplasm. In the nucleus, it trims the poly(A) tails of newly synthesized mRNAs to specific lengths (22) while the cytoplasmic fraction plays a role in mature mRNA deadenylation (12). Neither Pan2 nor Pan3 is essential for yeast growth (23,24) but their absence results in longer bulk poly(A) tails *in vivo*. In *Drosophila* Schneider cells Pan2 contributes to the deadenylation of the *hsp70* mRNA during recovery from heat shock (25). There is evidence that in mammalian cells, the Pan2/Pan3 deadenylase initiates cytoplasmic deadenylation (26).

After deadenylation, mRNAs can be degraded either unidirectionally from either end, or from both ends; the nature of the mRNA and the species determine which pathway predominates. Results from work in *S. cerevisiae* showed that the major pathway for degradation of some unstable deadenylated mRNAs is decapping, by a complex containing the MutT hydrolase Dcp2, then degradation by the 5′→3′ exonuclease Xrn1 (27–29). Alternatively, or in addition, deadenylated transcripts can be degraded by 3′–5′ exonucleases associated with the exosome (30,31); in this case the residual cap structure is degraded by the scavenger decapping enzyme DcpS (32). Computer modelling of mRNA degradation in yeast indicated that modulation of deadenylation has a stronger effect on mRNA half-life and levels than changes in decapping or the 3′–5′ and 5′–3′ decay pathways (33). Mammalian mRNAs that are destabilized by AU-rich elements (ARE) in the 3′-untranslated region (UTR) are subject to accelerated deadenylation (34–36) followed by digestion by 5′–3′ and 3′–5′ pathways (37,38). 5′ degradation is also important in *Drosophila* cells (25). In contrast, the stability of the alpha globin mRNA depends on binding of a complex that inhibits 3′–5′ decay (39). The 3′ pathway has also been shown to be important during degradation of mammalian mRNAs with premature termination codons (nonsense-mediated mRNA decay, or NMD) (40–42). In mammalian cells, the decapping enzyme, Xrn1, Dhh1, Pan2 and Caf1 co-localize in cytoplasmic processing bodies (P-bodies) (15) which are thought to be a site of mRNA decay.

Despite the importance of deadenylation, other deadenylation-independent mRNA degradation pathways clearly exist. First, degradation may be initiated by an endonuclease: examples include mammalian mRNAs subject to iron regulation (43), the alpha globin mRNA in mammalian erythroid cells (44) and the albumin RNA in *Xenopus* hepatocytes (45). In *Drosophila* and mammalian cells some mRNAs with premature termination codons (PTCs) are also attacked by an endonuclease (46–48). In yeast, RNAs with PTCs (49) and the mRNAs encoding the ribosomal protein Rps28b (50) and the decapping enhancer Edc1 (51) are subject to deadenylation-independent decapping. In contrast, degradation of mRNAs lacking a stop codon depends primarily on the exosome (52). Finally, degradation of mammalian histone mRNAs, which are not polyadenylated, is initiated by addition of poly(U) (53).

Trypanosomes are unicellular parasites which branched from the Opisthokont (fungi/animal) line very early in eukaryotic evolution (54). In trypanosomes, transcription by RNA polymerase II is polycistronic (55), individual mRNAs being generated by processing (*trans* splicing and polyadenylation) (56,57). Control of polymerase II initiation—even for the polycistronic units—has not been documented. Nevertheless, gene expression is regulated in order to allow trypanosomes to survive and grow in the mammalian host (the 'bloodstream form') and in the digestive tract of the Tsetse fly (the 'procyclic form') (58). To regulate gene expression, trypanosomes are therefore heavily dependent on mRNA degradation. The stability of trypanosome mRNAs is—as in other eukaryotes—determined mainly by sequences in the 3′-UTR (59). We have previously shown that degradation of relatively stable, constitutively expressed mRNAs depends on CAF1 activity (14). (Trypanosomes lack CCR4.) Trypanosome extracts possess decapping activities (60), but the proteins involved have not been identified. Of four XRN homologues, only XRNA has so far been shown to play a role in mRNA decay (61). Trypanosome XRNA and DHH1 are found in P-bodies (62).

Our previous work on degradation of highly unstable, developmentally regulated mRNAs has focussed mainly on two mRNAs that are highly expressed in the procyclic form trypanosomes, *EP* and *PGKB*. The *EP* mRNAs encode the major surface proteins of procyclic cells, the EP procyclins. Pairs of procyclin genes are arranged in a tandem repeat which is transcribed by RNA polymerase I (63). *EP* transcription is approximately 10-fold less efficient in bloodstream forms than in procyclic forms, most likely a consequence of epigenetic control (64). The *EP* mRNAs have a half-life of about 5 min in bloodstream-form trypanosomes, and over an hour in procyclic forms (65). Regulation of procyclin protein expression is completed by blocks to translation and protein processing (66). *PGKB* encodes a cytosolic phosphoglycerate kinase that is specific to procyclic forms; it is co-transcribed with the *PGKC* mRNA, which encodes a phosphoglycerate kinase that is abundant in bloodstream forms (56). The results of mathematical modelling indicate that mRNA stability is the major determinant of PGKB and PGKC expression (67).

Chloramphenicol acetyltransferase (CAT) reporter mRNAs with 3′-UTRs of either *EP* procyclin mRNA (*CAT-EP*) or *PGKB* mRNA (*CAT-PGKB*) are very unstable in bloodstream forms, with half-lives of around 5 min (68–70). The CAT-EP reporter thus has the same half-life as endogenous EP mRNAs. The half-life of PGKB mRNA has not been measured accurately because of its low abundance (less than one molecule per cell), but available data suggests a value of around 5 min (67). Mutational analyses on both reporters identified a single-stranded poly(U) tract in the 3′-UTR that was required for mRNA instability (69–73). Analysis of the kinetics of *CAT-EP* mRNA degradation indicated that degradation occurs without accumulation of deadenylated intermediates, and that the RNA is destroyed by both 5′–3′ and 3′–5′ exoribonuclease activities (68).

Correspondingly, depletion of either the exosome (74) or the 5′–3′ exonuclease XRNA (61) delays degradation of the *CAT-EP* and *CAT-PGKB* mRNAs. The results of XRNA depletion are more dramatic, with general disruption of *PGKB* and *PGKC* regulation: steady-state *PGKB* mRNA increases in bloodstream forms, while *PGKC* mRNA appears in procyclics (61). Analysis of *CAT-EP* degradation intermediates also suggested action of both deadenylation-dependent and -independent mRNA degradation pathways. In this article we investigate the roles of trypanosome CAF1 and PAN2 in rapid mRNA degradation.

MATERIALS AND METHODS

Sequence alignments

To find *PAN2* and *PAN3* genes, we searched various genomes using BLASTp, with the *S. cerevisiae* PAN2 or PAN3 protein sequences as the query, and then used the top match (or matches) as queries for the *S. cerevisiae* genome. Protein sequences that yielded *S. cerevisiae* PAN2 or PAN3 as the best match were categorized as potential homologues. Sequence alignments were done using ClustalW, with DNAStar software. Functional motifs were found using Prosite and NCBI searches.

Trypanosome culture, RNAi and plasmids

Bloodstream form *Trypanosoma brucei* stably expressing the tetracycline repressor (pHD 1313) and T7 RNA polymerase (pHD 514) were grown, transfected and clonally selected as described (75). The plasmids used in this study are described in Table S1. For *CAF1* and *PAN3* RNAi the vector $p2T7^{TA\ blue}$ (75) was used to make dsRNA from opposing tetracycline-inducible T7 promoters. In the *PAN2* and *MEX67* RNAi constructs, an inducible RNA polymerase I promoter drove expression of stem-loops (76). The plasmids were linearized with *Not* I and transfected into bloodstream-form trypanosomes expressing the tet repressor and T7 RNA polymerase (77). Transfectants were selected with 10 μg/ml hygromycin. The RNAi was induced by adding 1 μg/ml tetracycline to the medium. Samples were taken after 18.5 h of *CAF1* RNAi induction or after 2–3 days after *PAN2* RNAi induction.

In situ V5 tagging was done using the V5 plasmid described in (78), while over-expression of open reading frames with two myc tags was done as in (79).

RNA preparation and blotting

To analyse mRNA decay the cells were treated with Sinefungin (final concentration 2 μg/ml) for 5 min then Actinomycin D was added (final concentration 10 μg/ml) (80). Total RNA was isolated using peqGold Trifast (peqLab, Germany). To remove poly(A) tails, 170 pmol oligo $d(T)_{20}$ was incubated with 10–12 μg total RNA at 42°C for 10 min, 5 U RNase H (New England Biolabs) and RNase H buffer were added and the mixture incubated for 40 min at 37°C.

To select polyadenylated RNA, oligo d(T) cellulose (GE Healthcare) was treated with 0.1 M NaOH and washed in RNA-binding buffer (20 mM HEPES pH 7.4, 5 mM EDTA, 0.4% SDS, 500 mM NaCl). A total of 20 μg RNA was dissolved in RNA denaturation buffer (20 mM HEPES pH 7.4, 10 mM EDTA, 1% SDS). The mixture was heated at 65°C for 10 min then put on ice. A 1.5× volume of RNA dilution buffer (20 mM HEPES pH 7.4, 800 mM NaCl) was added. The RNA was transferred to a tube containing 10 mg resuspended oligo d(T) cellulose and incubated for 10 min at room temperature. After centrifugation the supernatant contained the poly(A)– fraction. The oligo d(T) cellulose was washed three times with washing buffer (20 mM HEPES, pH 7.4, 5 mM EDTA, 0.5% SDS). Poly(A)+ RNA was eluted with water.

RNA was analysed by formaldehyde gel electrophoresis, blotting onto Nytran membranes (GE Healthcare) and hybridization with radioactive DNA (Prime-IT RmT Random Primer Labelling Kit, Stratagene) or antisense RNA (MAXIscriptT7/T3, Ambion) probes. Signals were measured using a phosphorimager and normalized relative to the signal from a *7SL* (signal recognition particle) probe. Northerns were stripped by brief boiling in 0.1% SDS; the efficacy of stripping assessed by phosphorimager, and any residual signals left to decay as necessary before re-use.

RNA half-lives were measured by plotting relative signal intensities using Kaleidograph (Synergy software), including only the segments of the time course that gave exponential decay curves (fitted with a linear correlation coefficient generally exceeding 0.9). To mathematically describe the half-life of the *EP* transcript, we used Microsoft Excel to build models, assuming the presence of one or two exponential decay components. Since XRNA depletion results in simple exponential kinetics (half-life about 12 min) we varied one half-life around this value. The other half-life was varied from 1.5 min upwards; the proportions of mRNA affected by each pathway were also varied. The root mean square deviation of the model from the data was calculated and the model with minimum deviation adopted.

Poly(A) tail lengths were analysed as described previously (14). For pooled statistical analysis of time points 5 min, 15 min and 30 min, a Wilcoxon signed rank test was used (81).

Analysis of circular RNAs

RNA samples (60 μg, 400 μl) were treated with 40 units of DNase I (Invitrogen) with 240 units of RNaseOUT (Invitrogen) for 30 mins at room temperature. This and all following reactions were terminated by phenol-chloroform extraction and ethanol precipitation. To remove the terminal cap, ~10 μg of DNase-treated RNA was incubated with 2.5 units of Tobacco Acid Pyrophosphatase (TAP; Epicentre Biotechnologies) and 40 units of RNaseOUT (Invitrogen) in a 20 μl reaction for 1 h at 37°C. To remove the cap with the modified 5′ nt, 10 μg of DNase-treated RNA was incubated with 100 pmol of an oligonucleotide complementary to the

first 15 nt of the spliced leader (5′ TCTAATAATAGCGT T 3′) at 37°C in 33 µl of water. We than added 5 µl (1× RNase H buffer) of RNase H buffer, 1 µl (5 U) of RNase H and incubated for 1 h at 37°C. The RNA was extracted with phenol/chloroform and ethanol precipitated.

Circularization of 10 µg RNA was done in a reaction volume of 400 µl, using 40 units of T4 RNA ligase (New England Biolabs) and 80 units of RNaseOUT (Invitrogen), for 16 h at 16°C. For reverse transcription ~2 µg of RNA were incubated with 50 pmol of gene-specific reverse primer, 200 units SuperScript III RT (Invitrogen) and 40 units RNaseOUT (Invitrogen) in a 20 µl reaction. PCR amplification was performed in a 30 µl reaction [1 µl of cDNA (5%), 10 pmol each of forward and reverse primers, 2.5 units Taq DNA polymerase (New England Biolabs)] (30 s at 95°C, 30 s at 52°C and 45 s at 72°C). For the *RPL37A* mRNA, we used 38 cycles; for *EP*, each PCR was for 30 cycles. PCR products were purified and cloned into pGEMT-easy vector and randomly selected clones sequenced. Details of the oligonucleotides are in the Supplementary Data.

In situ hybridization

In situ hybridization followed approximately the protocols published previously (62,82). Gene-frames (Thermo scientific) were applied to glass slides, which were then coated with poly-L-Lysine. For each slide chamber, 10^6 to 10^7 cells were pelleted, washed with PBS, and fixed with 500 µl of freshly prepared 4% (w/v) paraformaldehyde for 18 min. Fixed cells were pelleted, washed three times in PBS, resuspended 200 µl PBS then allowed to settle on the slides overnight at 4°C. Cells were permeabilized with 0.2% (v/v) TritonX-100 in PBS (30 min), and washed three times with PBS. Total 50 µl hybridization buffer was added per chamber: 10× Denhardt's solution, 4× SSC, 1 mM EDTA, 35% deionized formamide, 0.5 µg/ml tRNA, 2 mU/ml RNase OUT. After 30 min 60 ng of 5′Cy3-oligo $d(T)_{30}$ was mixed with 10 µl of hybridization buffer and added to the hybridization mix. The chamber was covered with a coverslip, slides were heated to 65°C for 3 min., then incubated overnight at room temperature in a humid box. Coverslips and gene frames were removed and the slides were washed twice with 2× SSC (15 min), twice with 1× SSC (15 min) and twice with PBS (5 min). Cells were stained with DAPI solution (100 ng/ml, 15 min), washed twice with PBS (5 min) and allowed to dry for 1 h. Mounted preparations (Vectashield, Vector laboratories, H-1000) were viewed within 24 h.

Immunofluorescence

Totally 10^6 cells were fixed in 4% paraformaldehyde/PBS (w/v) for 20 min. The cells were allowed to settle on a poly-lysine coated glass slide (25 min), permeabilized with 0.2% (v/v) Triton X-100/PBS (room temperature, 20 min). Slides were blocked with 0.5% (w/v) gelatine (20 min), incubated with a 1:100 dilution of mouse α-V5 (Invitrogen) for 1 h, then a 1:500 dilution of the secondary antibody Alexa Fluor 488 goat α-mouse IgG (Molecular probes) for 40 min before repeated washing. The kinetoplast and the nuclear DNA were stained with 100 ng/ml DAPI/PBS for 10 min.

Cell fractionation

The fractionation method was taken from (83). A total of 2×10^8 cells were washed in PBS and resuspended in buffer A [150 mM sucrose, 20 mM KCl, 3 mM $MgCl_2$, 20 mM HEPES–KOH (pH 7.9), 1 mM DTT, complete EDTA-free protease inhibitor (Roche)]. Igepal CA-630 was added to a final concentration of 0.2%. The cells were passed three times through a 27 g needle. After a centrifugation (13 000 rpm, minifuge, 10 min) the supernatant (cytosolic fraction) was kept and purified by an additional centrifugation step, while the nuclear pellet was resuspended in buffer A and passed 15 times through a 27 g needle. The nuclear fraction was pelleted again (13 000 rpm, 10 min) and washed once more before use.

RESULTS

The trypanosome genome encodes potential homologues of PAN2 and PAN3

The trypanosome genome sequence encodes a single potential PAN2: the locus, Tb927.6.1670, is designated as a pseudogene in the 927 strain and is absent from the (incomplete) genome sequence of the 427 strain, but the gene is intact in other Kinetoplastid genomes (Figure S1). *Trypanosoma gambiense* and *T. brucei PAN2* genes are identical in all but 19 (out of 3256) nt, but a T at position 2697 in the *T. gambiense* sequence is missing in the corresponding *T. brucei* 927 sequence. To analyse the protein sequence we therefore restored this residue; sequencing of DNA from the 427 strain indeed revealed an intact open reading frame (M. Carrington and L. Ellis, University of Cambridge, personal communication).

Trypanosome PAN2, like the human and yeast proteins, has a C-terminal exonuclease III domain of the DEDDh RNase family (84), and this is the most conserved part of the protein: it is 38% identical to the equivalent portion of human PAN2. We compared the sequence with that of other, diverse eukaryotes (Figure 1; Figure S1 shows the complete alignment). The PAN2 of *Monosiga brevicollis*, the nearest unicellular relative to animals, retains all three domains, as do the PAN2s of *Chlamydomonas* and *Dictyostelium discoideum*. The *Chlamydomonas* sequence has mutations in putative active site and catalytic residues (20,84); for example, Asp 1083 was shown to be essential for activity of human PAN2 (20), but is missing in *Chlamydomonas* PAN2. *Aureococcus anophagefferens* (a chromalveolate alga), *Naegleria* (an amoeba), *Micromonas pusilla* (an alga related to green plants) and *Thalassiosira pseudonana* (a marine diatom) have truncated versions containing only the exonuclease domain (Figures 1 and S1), but in all of these apart from *Thalassiosira*, N-terminal active site residues are missing. We could not find PAN2 in *Arabidopsis*, *Plasmodium*, *Entamoeba*, *Trichomonas*, or *Giardia*: in these organisms the best match to PAN2 is another 3′–5′ exoribonuclease of *S. cerevisiae*, Rnh70, which is involved in maturation of 5S rRNA and tRNAs.

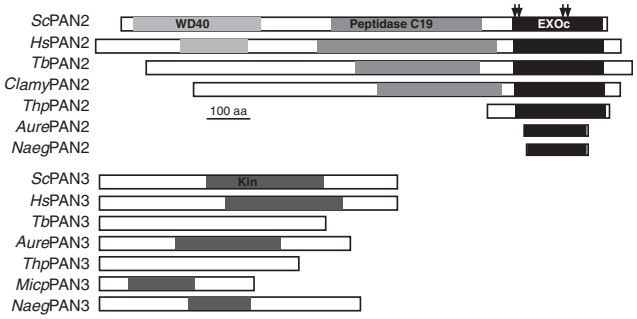

Figure 1. Cartoon maps of PAN2 and PAN3 from various species, as indicated on the left. Domains recognized by Prosite are also shown. Sc: *Saccharomyces cerevisiae*; Hs: *Homo sapiens*; Tb: *T. brucei*; Clamy: *Chlamydomonas reinhardtii*; Thp: *Thalassiosira pseudonana*; Neig: *Naegleria fowleri*; Aure: *Aureococcus anophagefferens*; Micp: *Micromonas pusilla*. EXOc is the exoribonuclease domain; 'Kin' is the putative kinase domain. The downward arrows indicate the approximate positions of residues thought to be required for catalytic activity according to an NCBI domain search and specifications for the cd06143 sequence cluster [e.g. (114,115)]. Complete sequence alignments are provided as Figures S1 (PAN2) and S2 (PAN3).

The WD40 repeat of the yeast and human PAN2s is missing from the trypanosome homologue. The central peptidase-C19 like domain—similar to ubiquitin hydrolases—was 27% identical to the human PAN2 peptidase domain and was recognized using default settings of the NCBI domain recognition algorithm, but the score was low ($E - 5 \times 10^{-6}$) and the domain was not recognized by Prosite. Moreover, in the putative *Tb*PAN2 peptidase domain, two of the three conserved active site residues (85) are mutated (C→K, H→D). Thus *T. brucei* PAN2 is unlikely to have ubiquitin hydrolase activity.

A search of the trypanosome database for PAN3 yielded Tb11.01.5540. For the potential PAN3 sequences found in a multi-organism search, sequence identities varied between 20% and 30% (Figures 1 and S2). A central kinase-like domain (SSF56112) was recognized in some proteins but not others; the role of this domain is unknown. The PABP-binding regions of yeast and human PAN3 are at different positions in the proteins, and are not sufficiently similar to enable us to determine whether such a region is conserved in the trypanosome protein. Interestingly, three organisms with truncated versions of PAN2 had a candidate PAN3; but we could not find it in *Thalassiosira, Monosiga, Chlamydomonas* or *Dictyostelium*, or in the organisms that lacked PAN2. Although some searches may have failed because the genomes were not 100% complete, and alternative algorithms might yield additional PAN2 and PAN3 sequences, the results so far indicate that both PAN2 and PAN3 have been lost several times in eukaryotic evolution.

Trypanosome PAN2 is in the cytoplasm and is required for normal growth

To find the location of PAN2, we integrated a sequence encoding a V5 epitope tag immediately upstream of the gene, to create an N-terminal fusion. The resulting V5-tagged protein was mostly in the cytoplasm by both immunofluorescence (Figure 2A) and cell fractionation (Figure 2B). We inducibly expressed PAN3 with a C-terminal myc tag; this was also in the cytoplasm (data not shown). Because the signals were weak in comparison with that from DHH1, we were unable to check whether PAN2 or PAN3 were in P-bodies. Preliminary results using co-immunoprecipitation suggested that a small proportion of the PAN3-myc was associated with V5-PAN2 (data not shown). Unfortunately, expression of PAN3-myc was rapidly lost during cultivation of the cell line, precluding further analysis. Attempts to tag the *PAN2* gene *in situ* with a TAP tag failed, and we have so far been unable to express PAN2 in *E. coli*.

We made several different trypanosome lines with tetracycline-inducible RNA interference targeting *PAN2* or *PAN3*. Induction of *PAN3* RNAi did not affect growth (data not shown). In contrast, cells with *PAN2* RNAi showed variable levels of growth inhibition. Figure 2C shows cultures that ceased growth completely after PAN2 depletion, whereas the line illustrated in Figure 2D were less affected; another line (data not shown) had a division time of 6.7 h without tetracycline and 8.2 h after RNAi induction. All lines rapidly lost RNAi upon either storage or propagation, and some grew slowly in the absence of tetracycline, suggesting leakage of the RNAi. These problems, which are common in trypanosome clones with detrimental inducible RNAi, prevented us from conducting extensive series of experiments with individual inducible cell lines.

From these experiments, we concluded that PAN2 is in the trypanosome cytoplasm, is probably required for optimal growth, and might be essential. It is not clear whether, in trypanosomes, PAN2 is stably associated with PAN3, and we have no evidence that PAN3 is required for PAN2 function.

Depletion of PAN2 decreases deadenylation

To find out whether PAN2 is important for mRNA deadenylation in trypanosomes, we measured bulk poly(A) tail lengths in cells with or without RNAi, and after inhibition of transcription. Cells with *PAN2* RNAi reproducibly had more poly(A), as judged by the signals on the autoradiograms (Figure 3A). Although equal amounts of starting RNA were used for each reaction, this effect cannot be quantitated accurately because the design of the assay precludes inclusion of a loading control. Instead, to measure the effect of RNAi, we analysed the distributions of poly(A) tail lengths within each sample (Figure 3B). At steady state (time = 0), there was no significant difference in poly(A) tail lengths between the normal and PAN2-depleted cells, but after transcription inhibition, deadenylation was delayed. Quantitation of the relative intensities of the signals for short (0–15), intermediate (51–100) and long (101–200) poly (A) tails revealed that after 5, 15 and 30 min of transcription inhibition, the samples from PAN2-depleted cells had longer poly(A) tails than samples from the normal cells (Figure 3B). The effect was weaker than that seen upon depletion of CAF1 (14). This could indicate that PAN2 has a minor role in deadenylation of all mRNAs, or that it attacks only a subset of mRNAs. It is also possible that the weakness

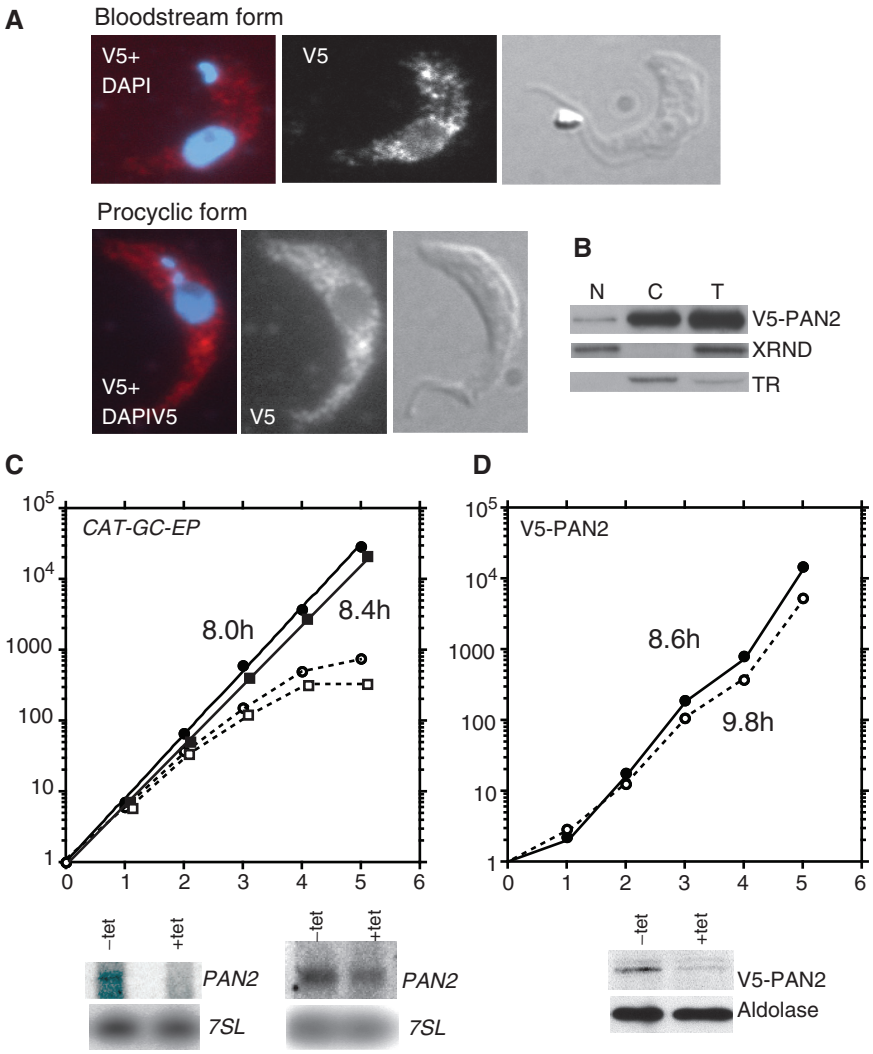

Figure 2. PAN2 is mainly in the cytoplasm and RNAi inhibits trypanosome growth. (**A**) In bloodstream-form or procyclic-form trypanosomes, one *PAN2* allele was tagged *in situ* at the N terminus with a sequence encoding a V5 tag. The tag was detected by immunofluorescence. DAPI staining shows the positions of the nucleus (large spot) and kinetoplast DNA (small dot). A phase-contrast image of the trypanosome is on the right. (**B**) Detergent lysates (T) from the V5-tagged cells were separated into nuclear (N) and cytoplasmic (C) fractions and proteins detected by western blotting. XRND: nuclear exoribonuclease (61); TR: trypanothione reductase. (**C**) *PAN2* RNAi inhibits trypanosome growth. Results for two bloodstream-form cell lines are shown; each expresses the tet repressor and T7 polymerase (1313-514) and has an integrated copy of the PAN2 RNAi plasmid. Cells were grown with (open circles, dashed lines) or without (closed circles) tetracycline added at day 0, and were diluted as required. Cumulative growth curves are shown, with doubling times calculated from exponential curves (Kaleidograph). The results are for two lines expressing the *CAT-GC-EP* reporter. The panels beneath are northern blots probed for *PAN2*, with *7SL* as a control. In the right hand panel, *PAN2* mRNA was only depleted by 30%, but the cells nevertheless showed growth inhibition. (**D**) RNAi in cells with V5 *in situ* tagged PAN2, details as in (C). The panel below is a western blot that was probed with antibody to the V5 tag and to aldolase.

of the effect is caused by persistence of PAN2 protein after RNAi induction.

We previously showed that *CAF1* RNAi strongly inhibits degradation of constitutively-expressed trypanosome mRNAs, such as those encoding glycosomal PGKC, histone H4 (HISH4), tubulin (TUB) or actin (ACT) [(14) and see also Figure 4A]. PAN2 depletion, like CAF1 depletion, did not cause an increase in steady-state levels of these mRNAs (Figure 3D and E, and data not shown). PAN2 depletion had no significant effect on *HISH4* (Figures 3D) or *TUB* (Figure S3) mRNA decay. In Figure S3 we show the mRNA degradation curves normalized to wild-type, so that any effects of RNAi on in steady-state mRNA levels are apparent. *ACT* RNA was slightly more stable in PAN2-depleted cells (Figure 3C and E). This effect was clearest 30 min after RNA synthesis inhibition: at this time point, in five out of five experiments, there was more mRNA left in the RNAi-induced cells than in the controls. At 60 min, *ACT* mRNA was undetectable in the control samples but detectable in the RNAi samples. We concluded that PAN2 depletion affected decay of the *ACT* mRNA.

Deadenylation plays a role in degradation of the unstable *EP* mRNA

We previously showed that RNAi targeting the 5′–3′ exonuclease XRNA in bloodstream forms caused accumulation of the unstable *EP* procyclin and *PGKB*

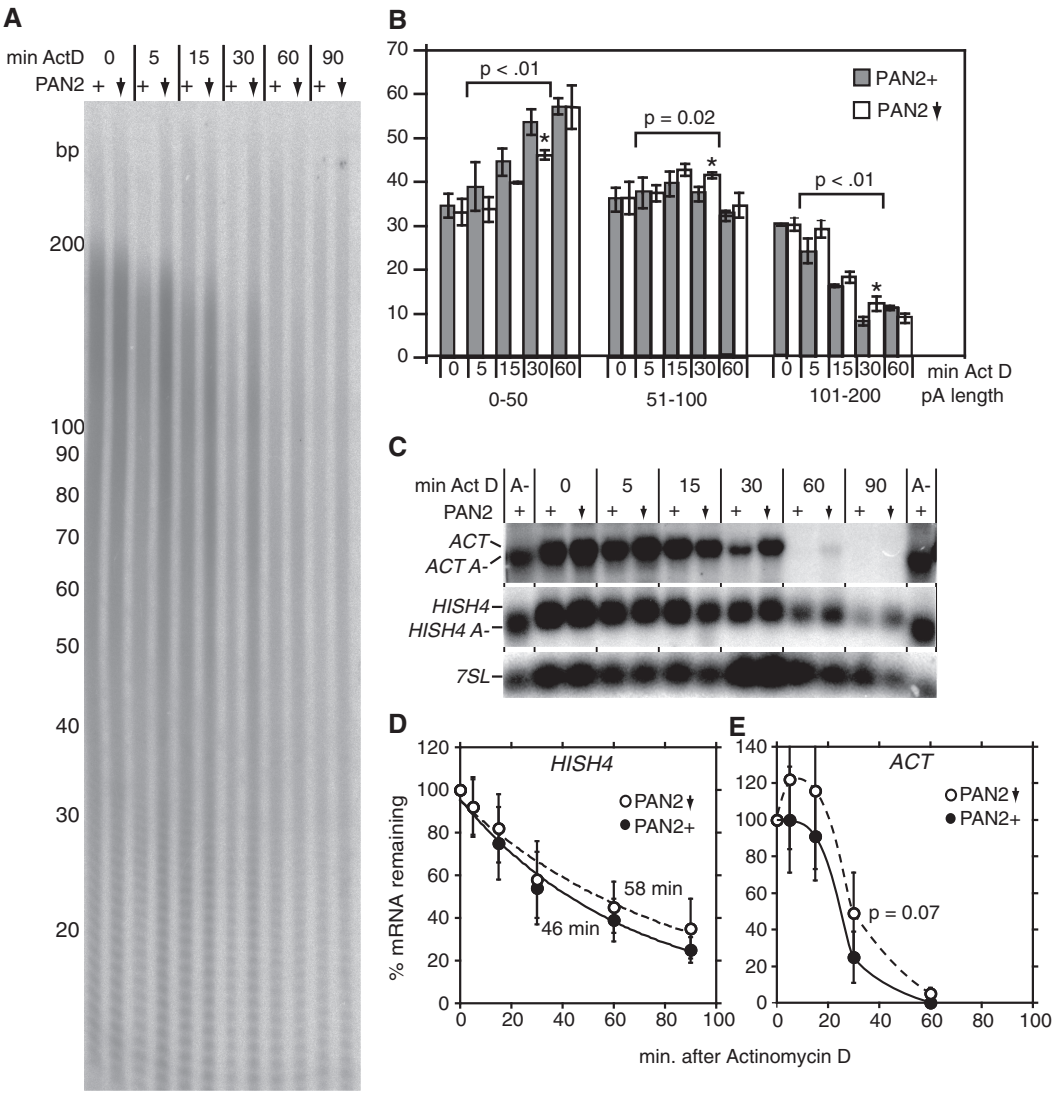

Figure 3. PAN2 depletion inhibits deadenylation. (**A**) Trypanosome RNAs were 3′ labelled with [^{32}P]-pCp then digested with RNase T1 and RNase A to leave the poly(A) tails. The resulting RNA was separated on a denaturing polyacrylamide gel and the [^{32}P] was detected using a phosphorimager. The downward arrows indicate depletion of PAN2 by RNAi. The '+' sign indicates that PAN2 is present (RNAi line in the absence of tetracycline). (**B**) Quantitation of (A). The poly(A) tails were divided into three size classes, as indicated on the right, and the signal from each class measured. The proportion of each class, relative to the total signal on the relevant lane, was then measured. This quantitation minimizes the effect of PAN2 depletion since it does not show the differences in total signal intensity between lanes. Results are the arithmetic mean of three independent measurements with standard deviations. Individual sets of three measurements that were significantly different in a Student's *t*-test ($P < 0.05$, 30-min time points) are shown with asterisks. The results for 5 min, 15 min and 30 min were also pooled and compared using a Wilcoxon ranking test (see numbers above the lanes). Tails of 0–50 nt were less abundant in the PAN2 RNAi samples than in the control in 15/15 cases, giving a *P*-value of <0.01. The longer tails of 51–100 nt and 101–200 nt were more abundant in the *PAN2* RNAi samples (*P*-values of 0.02 and <0.01, respectively). (**C**) Northern blots showing amounts of various mRNAs after inhibition of mRNA synthesis. Sinefungin was added at time –5 min, and Actinomycin D was added at time = 0. *ACT*: actin; *HISH4*: Histone H4; *7SL*: RNA of the signal recognition particle. Lanes labelled A- contain RNA that was incubated with oligo d(T) and RNase H before loading. Signals were detected and measured using a phosphorimager, using the *7SL* RNA as a loading control. (**D**) Quantitation of results for the *HISH4* mRNA. Means and standard deviations for four independent measurements are shown, with fitted exponential degradation curves (Kaleidograph) and corresponding half-lives. For quantitation of all measurements relative to wild-type values see Figure S3. (**E**) Quantitation of results for the *ACT* mRNA. Means and standard deviations for five independent measurements are shown. The result of a Student's *t*-test for the 30-min time point is indicated on the graph. The differences at 30 min were also significant ($P < 0.02$) in the Wilcoxon ranking test.

mRNAs. In addition, a role for deadenylation was indicated by the existence of deadenylated *EP* and *CAT-EP* mRNA (61,74). We therefore analysed the effects of both CAF1 and PAN2 depletion on *EP* mRNA turnover. *HISH4* mRNA was included as a control for deadenylation inhibition in the *CAF1*-depleted cells.

After inhibition of transcription, in cells without RNAi induction, *EP* procyclin transcripts showed an initial rapid decrease, followed by a slower phase (Figure 4A). The kinetics could be explained by the existence of two exponential decay components: about half of the RNA had a half-life of around 2 min and the rest, a half-life of 14 min. After *CAF1* RNAi, the abundance of *EP* transcripts

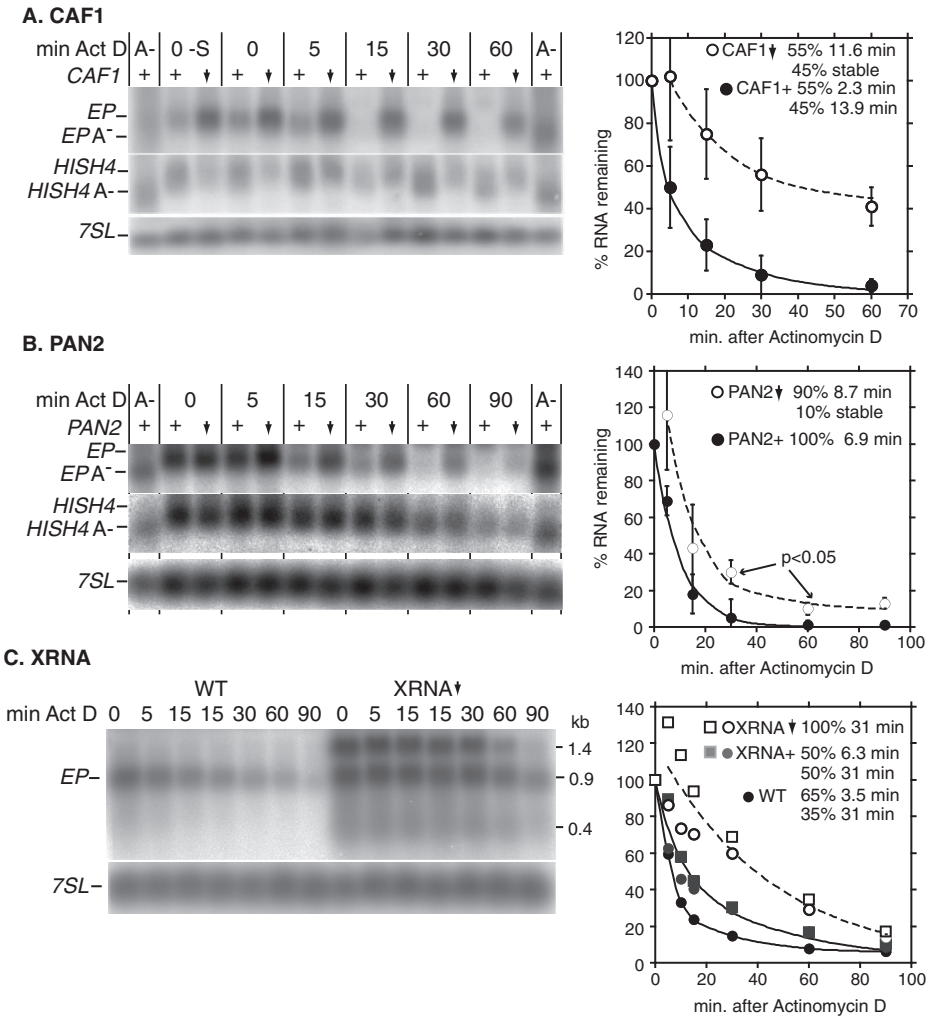

Figure 4. Degradation of trypanosome *EP1* mRNA is effected by deadenylation-dependent and -independent pathways. (**A**) mRNA synthesis was inhibited with Sinefungin and Actinomycin D in cells with inducible *CAF1* RNAi, either without tetracycline or 18 h after tetracycline addition. Total RNA was prepared and the abundances of specific transcripts analysed by northern blotting. A typical blot is shown. Quantitation is on the right. Results are arithmetic mean and standard deviation for four independent experiments. The fitted lines were determined by assuming the presence of two exponential decay components and minimising deviation from the experimental observations (see Methods section). The parameters used to fit the curves are indicated as half-life in min, and the proportion of the RNA with that half-life. (**B**) As for A, but using cells with RNAi targeting *PAN2*. Results are for three experiments, and *P*-values from a Student's *t*-test for the 30 min and 60 min time points are shown. (**C**) Degradation kinetics of *EP* mRNA in cells with normal or depleted *XRNA*. Data points for two independent experiments are shown, with a different symbol for each experiment. For the wild-type (no integrated RNAi construct), one experiment was included as a control. The curves are fitted to the arithmetic mean values.

increased 1.2- to 3.1-fold, and their degradation was inhibited (Figures 4A and S3B). After *CAF1* depletion, the degradation kinetics were best explained by a model in which half of the RNA was degraded with a half-life of 12 min and the remainder had a half-life of over 8 h: even after 90 min, 45% of the *EP* mRNA persisted. From these kinetics, it appeared that half of the *EP* mRNA is degraded by a pathway that depends on CAF1.

In the *PAN2* RNAi cell line, *EP* mRNA had a half-life of about 7 min in the absence of RNAi induction, suggesting some inhibition of degradation because of RNAi 'leakage'. With *PAN2* RNAi, degradation was further inhibited and 10% appeared to be stable (Figures 4B and S3A). These results suggest that PAN2 is required for optimal *EP* mRNA degradation. We cannot make any judgements concerning the relative importance of the two deadenylases in *EP* mRNA degradation since we do not know the extents of PAN2 and CAF1 depletion and—even if we did—we do not know the threshold below which depletion might have an effect. Digestion with oligo d(T) and RNaseH increased the mobility of *EP* mRNA, suggesting the presence of a poly(A) tail of at least 50 nt (Figure 4A and B).

We had previously shown that *XRNA* RNAi inhibited the degradation of a *CAT-EP* reporter mRNA. We now examined the effect of *XRNA* RNAi on *EP* mRNA degradation (Figure 4C). The graph quantitates the ~900-nt mature *EP* mRNA. Degradation in cells without the RNAi construct was biphasic as expected. Uninduced *XRNA* RNAi cells showed a slight retardation of the degradation, relative to wild-type cells, and *XRNA* RNAi eliminated the fast degradation component.

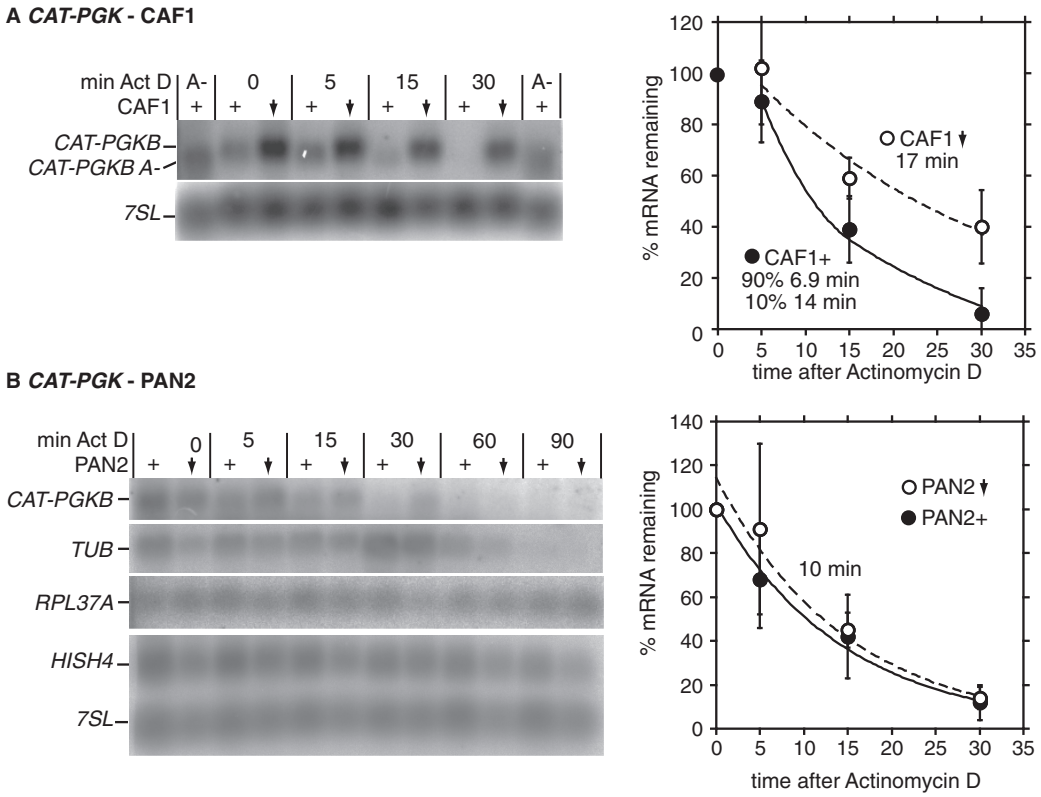

Figure 5. Depletion of CAF1 or PAN2 has minor effects on degradation of *CAT-PGKB* mRNA. (**A**) Northern blot illustrating *CAT-PGKB* mRNA degradation in cells depleted of CAF1. Details as in Figure 4A, three experiments. (**B**) Northern blot illustrating *CAT-PGKB* mRNA degradation in cells depleted of PAN2. Details as in Figure 4B.

Modelling using our previous data for the *CAT-EP* mRNA (61) yielded almost identical results to those for *EP* (Figure S4A).

Surprisingly, northern blots of RNA from cells containing the *XRNA* RNAi construct had, in addition to the expected band at 0.9 kb, two additional bands: one at 1.3 kb and one at about 0.4 kb. These were faint, but detectable, in RNA from cells grown without tetracycline (data not shown) and clearly visible after RNAi induction (Figure 4C). Both hybridized with an *EP* probe containing only the coding region; the shorter product was not detected in the poly(A)+ fraction (data not shown) and could be a coding region fragment. The longer product was polyadenylated; a band of similar size hybridized to an intergenic region probe (data not shown). This RNA is too long to be a polyadenylated primary transcript, but could be a previously detected minor alternatively spliced version of *EP2* or *EP3* mRNA, extended at the 5′-end (86,87). Thus XRNA seems to be implicated in destruction of abnormal, probably non-functional mRNAs from the procyclin locus.

These results indicate that extremely rapid degradation of *EP* mRNA requires XRNA, but some *EP* mRNA is degraded by a pathway that depends on the presence of CAF1.

Degradation of the *CAT-PGKB* and *PGKB* mRNAs

The endogenous *PGKB* mRNA, produced by pol II, is virtually undetectable by Northern blotting. Even using real-time PCR, the levels were only just above the detection limit, making accurate quantitation impossible (data not shown). The only conclusion we could make was that as for other polymerase II transcripts, the steady-state level of *PGKB* mRNA did not appear to have been changed by CAF1 depletion. The mRNA level dropped below the real-time PCR detection limit 5–15 min after inhibition of mRNA synthesis so the degradation rate could not be measured. In order to obtain sufficient mRNA for analysis, we therefore investigated the effects of deadenylase depletion in cell lines expressing the *CAT-PGKB* reporter mRNA from an RNA polymerase I promoter. The *CAT-PGKB* mRNA has a half-life of 5–7 min (70,74). Depletion of CAF1 resulted in modest stabilization (Figures 5A and S3B). In two experiments with a *PAN2* RNAi cell line, we also saw stabilization of *CAT-PGKB* mRNA (see for example upper panel of Figure 5B) but this was not seen in two further experiments. Thus the role of PAN2 in *CAT-PGKB* mRNA degradation is uncertain. From these results we concluded that deadenylation plays a minor role in degradation of *CAT-PGKB* mRNA.

TbCAF1 depletion partially inhibits 3′→5′ degradation of *CAT-EP* mRNA

To examine the various degradation pathways for *CAT-EP* in more detail, we depleted CAF1 in a cell line expressing a *CAT-GC-EP* reporter, which has a $C_{30}G_{30}$ sequence between the *CAT* ORF and the *EP* 3′-UTR (61,68,74). The $C_{30}G_{30}$ causes stalling of exoribonucleases.

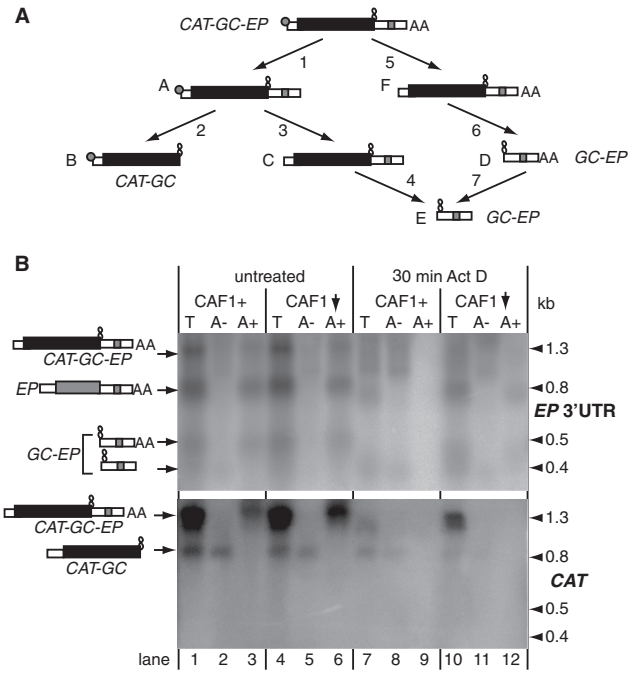

Figure 6. Degradation of the *CAT-GC-EP* reporter mRNA in trypanosomes. (**A**) Possible pathways of degradation. The *CAT-GC-EP* mRNA has, from 5′ to 3′, a cap (small circle), a short 5′UTR (white fill), a *CAT* open reading frame (black), a $G_{30}C_{30}$ sequence, then the *EP1* 3′-UTR (white, with destabilising 26-mer in grey) and poly(A) tail (AAAA). (1) deadenylation as the first step in degradation (product 'A'); (2) degradation of the deadenylated RNA from the 3′-end, pausing at the $G_{30}C_{30}$ sequence to produce the *CAT-GC* intermediate (product 'B'); (3) decapping of the deadenylated mRNA; product 'C', indistinguishable from 'A' by northern blotting; (4) degradation of product 'C' from the 5′-end, pausing at the $G_{30}C_{30}$ sequence to give the deadenylated 3′ *GC-EP* RNA (product 'E'); (5) decapping as the first step in degradation, to give product 'F', indistinguishable from the initial RNA by northern blotting; (6) degradation of product 'F' from the 5′-end, pausing at $G_{30}C_{30}$ to give a polyadenylated 3′ *GC-EP* RNA (product 'D'); (7) deadenylation of RNA 'D' to give RNA 'E'. (**B**) The effect of inducible *CAF1* RNAi on *CAT-GC-EP* mRNA degradation. CAF1+: cells without tetracycline; CAF1 with downward arrow: cells with tetracycline (19–21.5 h). Total RNA (T) was prepared and part of it was separated into poly(A)+ (A+) and poly(A)– (A–) fractions. The identities of the bands are shown on the left and sizes on the right. The upper panels were hybridized with an *EP* 3′-UTR riboprobe. This reproducibly cross-hybridizes with the smallest rRNA fragment. Although this signal has been cropped from the picture, it smears a little into the upper portions of the total and poly(A)– lanes. The lower panels are hybridizations with a *CAT* probe. The ratio of the *CAT-GC* fragment to the full-length mRNA fragment was measured in three experiments: for cells without tetracycline the average ratio was 21% (range 15–26%) and for *CAF1*-depleted cells 14% (range 12–16%). The degradation fragments were detected readily only if we probed for them first: the upper and lower panels therefore originate from different experiments.

The pathways that could be responsible for the various possible degradation intermediates [previously identified in (61)] are depicted in Figure 6A. A *CAT* probe detected the full-length *CAT-GC-EP* mRNA (Figure 6B, lane 1), which was recovered in the poly(A)+ fraction (Figure 6B, lane 3). Based on published analyses (88) we estimate that this fraction included RNAs with tails of greater than 20 nt. The *CAT* probe also detected a fragment containing the 5′-UTR joined to the *CAT* gene and terminating at the $C_{30}G_{30}$ sequence (*CAT-GC*); this was in the poly(A)– fraction as expected (Figure 6B, lanes 1 and 2). A probe for the *EP* 3′-UTR detected the polyadenylated *CAT-GC-EP* and *EP* procyclin mRNAs (Figure 6B, lanes 1 and 3). In addition, the *EP* probe detected two *GC-EP* 3′-end fragments, one of which was deadenylated (Figure 6B, lane 2) and one of which was, on average, about 100-nt longer and bound to oligo (dT) (Figure 6B, lane 3). The presence of the latter fragment suggests that 5′→3′ exonuclease is able to target an mRNA with a poly(A) tail longer than 50 nt (61). Meanwhile, the deadenylated *GC-EP* fragment could arise either from deadenylation of the complete *CAT-GC-EP* mRNA, followed by 5′→3′ degradation, or from deadenylation of pre-made *GC-EP* RNA fragments. Thirty minutes after addition of Actinomycin D, only shadows of deadenylated *EP*, *CAT-GC* and *GC-EP* RNAs remained (Figure 6B, lanes 7 and 8); the poly(A)+ lane (lane 9) was reproducibly empty.

We had previously shown that after XRNA depletion, a smear of *CAT-GC-EP* and *EP* mRNAs becomes detectable in the steady-state poly(A)– fraction, indicating stabilization of deadenylated mRNA [(61) and Figure S4B]. Exosome depletion had no effect on the pattern of intermediates at steady state, but partially stabilized deadenylated full-length *CAT-GC-EP* mRNA [(74) and Figure S4B]. Depletion of PAN2 did not result in any obvious change in the pattern of *CAT-GC-EP* mRNA degradation (data not shown). After depletion of CAF1, the only effect at steady state was in a slight decrease in the abundance of the *CAT-GC* fragment relative to the amount of *CAT-GC-EP* RNA (Figure 6B, lower panel, lanes 4 and 5; see figure legend for quantitation). This would be expected if the production of *CAT-GC* were initiated by deadenylation. 30 min after Actinomycin D addition full-length mRNA was more abundant after CAF1 depletion (Figure 6B, visible in lanes 7 and 10 hybridized with the *CAT* probe). More strikingly, the poly(A)+ lane (Figure 6B, lane 12) contained some *CAT-EP* mRNA, *EP* mRNA and the polyadenylated 3′ *GC-EP* fragment; in contrast, for CAF1+ samples, this lane was completely empty (Figure 6B, lane 9).

These results demonstrate the role of CAF1 in deadenylating the *CAT-GC-EP* and EP mRNAs, and in initiating 3′–5′ degradation.

Sequencing of uncapped mRNA reveals multiple degradation pathways

To more characterize endogenous mRNA degradation intermediates, we used an RNA circularization and sequencing strategy (89). In this procedure (Figure 7A), RNAs with a 5′-phosphate and 3′-OH group are diluted to a low concentration, then incubated with T4 RNA ligase to join the ends, creating circles. After that, the 5′–3′ junction is reverse transcribed, then amplified by PCR (Figure 7A). The products are subsequently cloned and sequenced. To sequence full-length mRNAs, the cap must be removed since capped 5′-ends cannot be ligated; the methylated nucleotides just downstream of the cap must also be removed because they inhibit reverse transcriptase (90–94). In order to obtain ligation products

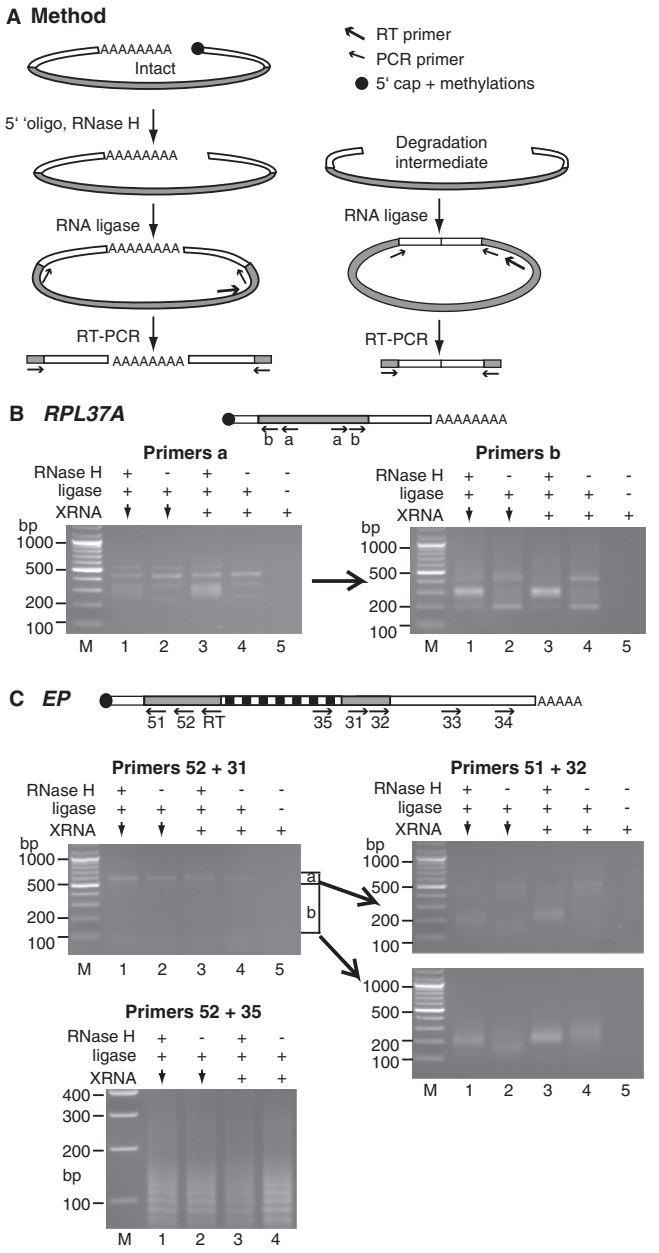

Figure 7. RT–PCR of circularized mRNAs. (**A**) Illustration of the method for intact, capped RNA (right) and a degradation intermediate (left). The open reading frame is filled grey, other symbols are shown on the figure. For detailed description see text. (**B**) Ethidium-bromide stained gels of amplified products for *RPL37A*. A cartoon of the mRNA, not to scale, showing the positions of the primers, is above the gels. Products from the first PCR (primers 'a') are shown on the left, and from the second, nested PCR (primers 'b') on the right. (**C**) Ethidium-bromide stained gels of amplified products for *EP*. In the cartoon, the striped region represents the segment encoding EP repeats. After the first PCR with primers 52 and 31, DNA was isolated from the upper and lower portions of the gel, as indicated, and used for the nested PCR using primers 51 and 32. A separate picture shows the ladders obtained using primers 35 and 52. In each case, the area of the gel containing most DNA was excised for purification and cloning of the PCR products, and clones were selected randomly for sequencing. Gels for amplifications with 3′ primers 33 or 34, with 5′ primer 51, looked very similar to the lower panel for primers 51 and 32; the same procedure was followed but only clones with the longest inserts were sequenced.

from mRNAs with intact 5′-ends and cap structures, we therefore pre-incubated samples with RNase H and an oligonucleotide complementary to the 5′-end of the spliced leader. When considering the results, it is important to note that if an mRNA had been decapped *in vivo*, but still retained the 5′ methylated nucleotides, it would be detected only in RNase H treated samples. Such decapped RNAs are expected to accumulate after XRNA depletion.

Tandemly repeated precursor RNAs should be substrates for RNA-ligase-independent amplification, and are expected for both *HISH4* and *TUB*. We therefore chose, as a control, the ribosomal protein L37a mRNA (*RPL37A*), which is encoded by a single locus, has a predicted length of about 400 nt, and has a half-life exceeding 90 min in bloodstream-form trypanosomes (Figure 5B). RNA circle results for *RPL37A* are shown in Figure 7B, and sequencing results for a random selection of cloned products are in Tables 1 and S2, and Figure S5. The mRNA is *trans* spliced at a single site, but there are several alternative polyadenylation sites. Figure 7B shows the products of the RT–PCRs. The first PCR showed a ladder in all lanes, except for the negative control without ligase (lane 5). In lanes 1 and 3, showing products from 5′ RNase H-treated RNA, there was a broad band around 300 nt, which was absent in the products from RNA that had not been RNase H treated. The predicted length for amplification products without the poly(A) tail was 159–210 bp, so the size of this band suggested average poly(A) tail lengths of about 100 nt. Cloning, however, instead gave poly(A/T) tracts of 36–37 bp. In the original article describing the method (89), the poly(A) tails of four rat mRNAs were measured by gel electrophoresis, without cloning. Amplification of three of them indicated poly(A)s of 20–50 nt; for one mRNAs there were two populations, corresponding to 20–50 nt and 120–200 nt. Since mammalian poly(A) tails are expected to be 100–200 nt long, these results hint that the circle–PCR method may have an intrinsic bias against longer poly(A) tails. Our results show that the bias is exacerbated if the products are cloned.

RPL37A products from RNA that had not been treated with RNase H were expected to correspond to mRNAs that had already been decapped and had begun to be degraded from the 5′-end: they formed a smear in the agarose gel (Figure 7B). In order to reduce contamination with irrelevant cDNAs prior to cloning, we performed a nested PCR. Surprisingly, the 5′-ends of the degradation intermediates were not random. Instead, 25 out of 46 clones had lost the first 27–31 nt of the spliced leader. About half of the degradation intermediates had lost the poly(A) tail and parts of the 3′-UTR as well. In contrast to observations for mammalian histone RNAs (53), here was no evidence for addition of U residues at the 3′-ends of the degrading mRNAs. Depletion of XRNA did not affect the patterns of degradation products. If poly(A) tails were present they were almost always in the 30–40 nt size range. Because of the bias noted earlier, this result gives us the lower limit of poly(A) lengths for deadenylation-dependent decapping, but does not tell us the upper threshold. Just 2 of the 43 cloned intermediates had much

Table 1. Summary of results for circularized RNAs

Gene	RNaseH	XRNA	#	Nt 5′	nt 3′	pA (%)	(A)n
RPL37A full				*55*	*108–136*		
RPL37A circles	+	+	5	38 ± 4	108, 127, 136	100	36 ± 4
	−	+	23	27 ± 8	78 ± 42	43	44 (5–93)
	+	−	5	39 ± 4	108,136	100	36 ± 5
	−	−	20	20 ± 15	97 ± 37	50	34 (5–112)
EP full				*70*	*312*		
EP circles	+	+	8	49 ± 25	37 ± 22	62	7 (3–11)
	−	+	23	38 ± 33[a,*]	29 ± 35	59	12 (3–28)
	+	−	8	57 ± 1	28 ± 22	12	10
	−	−	16	−11 ± 28*	76 ± 98	19	5 (4,5)

Results are shown for products of *RPL37A* amplified with the 'b' primers (Figure 7B) and for *EP* mRNAs amplified with 5′ primers 51 or 52, and 3′-primer 32 (Figure 7C). 'RNase H'—removal of 5′-end of *SL* by RNase H digestion; 'XRNA'—presence of normal XRNA (+) or depleted XRNA (−). # denotes number of clones sequenced; in each case, clones with various insert lengths were selected. Results for 5′ and 3′ ends (nt 5′, nt 3′) are the numbers of nucleotides beyond the ATG start codon or the stop codon, respectively, expressed as arithmetic mean ± SD, including clones with and without poly(A). The lengths for full-lengths RNA are given for reference ('full') and are shown in italics. 'pA' shows the percentage of clones that had a poly(A) tail. The '(A)n' lane indicates the arithmetic mean lengths of poly(A) tails, where present, with either the standard deviation or the range.

[a]Not including the primary transcripts.

*Significantly different, $P < 0.001$ (*t*-test).

longer poly(A) tails (93 nt and 112 nt), illustrating the minor role of deadenylation-independent decay.

We next repeated the experiment for *EP* mRNA. In bloodstream forms, at steady state, *EP* mRNAs have a poly(A) tail of at least 50 nt, added about 300-nt downstream of the stop codon (e.g. Figures 4 and 6B, lanes 2 and 3). Primers 52 and 31 (Figures 7C and S6) were designed to allow detection of a broad range of degradation products, including those that had lost long segments of the 5′ and 3′-ends. First, we examined RNase H-treated mRNA, in order to see the full-length mRNA. The corresponding amplified product should have been 430 bp plus poly(A). To our surprise, a band of this size was not seen and no clones corresponding to full-length mRNA were obtained. Instead, the RNase H-treated RNA yielded *EP* products that were predominantly in the 200 bp range (Figure 7C, lanes 1 and 3). Randomly selected clones nearly all retained *SL* sequence, but either lacked a poly(A) tail, or had $(A)_{3–11}$ at positions over 100-nt upstream of the usual site (Tables 1 and S3, and Figure S7).

We next amplified *EP* cDNAs using RNaseH-treated RNA from XRNA-depleted cells with primers 52 and 31. The average size of the products was shorter than before (Figure 7B, compare lane 1 with lane 3). Although all eight cloned products had retained the expected portions of the spliced leader, only one of them had a poly(A) tail (Table S3 and Figure S7). This illustrates stabilization of deadenylated *CAT-EP* mRNA after XRNA depletion (61)

To find out whether the procedure could amplify full-length *EP* mRNA from bloodstream forms at all, we repeated amplifications with primers 33 and 34 and selected only the longest inserts for sequencing (Table S4 and Figure S8). The product distributions on agarose gels were similar to those obtained with the first primer sets (data not shown). Even with primer 34, no clones had poly(A) in the expected position, although one was polyadenylated a few nucleotides further downstream (Figure S8). This result is strange, since it is inconsistent with the northern blot results. It will not be discussed further here, because a considerable number of further experiments is required to determine the origin of these products. In procyclic forms, the *EP* mRNA is very stable and polyadenylated. In preliminary experiments with RNaseH-treated mRNA from this form, using primers 33 and 34, 6 out of 12 clones were polyadenylated in the expected position at +297, with an average poly(A) length of 29 nt (maximum 58 nt). This shows that the procedure can indeed amplify the full-length polyadenylated RNA, but probably biases towards shorter products and truncates the tails.

Returning to the bloodstream-form trypanosomes, we next analysed circularized *EP* mRNAs without prior RNAase treatment. Using RNA from cells with normal XRNA levels, approximately half of the amplified products using 3′ primer 32 had an oligo(A) tail, well upstream of the expected position; the intermediates without poly(A) had lost variable portions of the 3′-UTR. It was obvious on the stained agarose gel that products from cells with *XRNA* RNAi (Figure 7C, lane 2) were smaller than those obtained from cells with a normal amount of XRNA (Figure 7C, lane 4). The clones from the XRNA-depleted cells mostly lacked poly(A) and had been digested significantly further at the 5′-end than those from the normal cells: 56% had lost part of the coding region, and only 1/18 had retained part of the spliced leader, while in XRNA positive cells, 14% had lost coding sequence and 64% retained part of the spliced leader. Surprisingly although the coding region primers were designed to hybridize equally to *EP1*, *EP2* and *EP3* sequences, all clones originated from *EP1*. Two clones (no RNase H, normal XRNA) originated from the primary transcript, enabling precise mapping of the transcription start site at position −115 relative to the start codon.

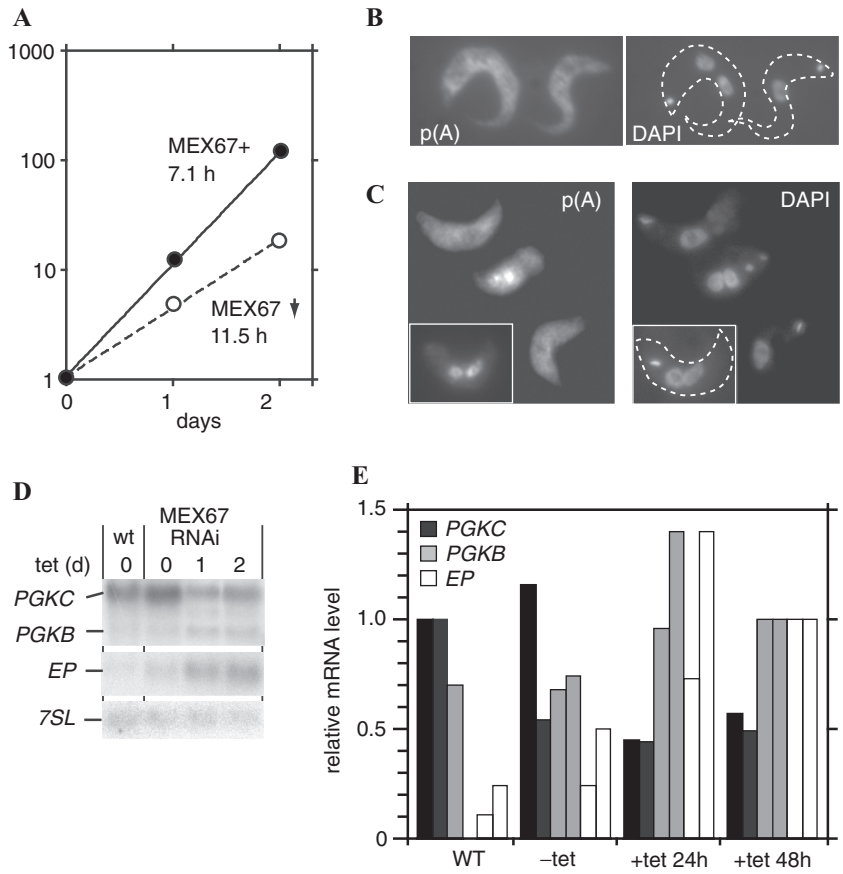

Figure 8. (**A**) RNAi targeting *T. brucei MEX67* inhibits growth. A cumulative growth curve is shown. (**B** and **C**) RNAi targeting *T. brucei MEX67* results in accumulation of poly(A)+ RNA in the nucleus. Cells without an RNAi construct (B) or cells with inducible RNAi (C) were incubated with or without tetracycline for 48 h. poly(A) was detected in the cells by *in situ* hybridization (p(A)). The DNA stain (DAPI) is on the right; some outlines of the parasites are added (dotted lines) to facilitate interpretation. (**D**) Effect of MEX67 RNAi on mRNA levels. RNA was prepared at the indicated times after tetracycline addition and *EP, PGK*, and *7SL* mRNAs were detected. (**E**) Quantitation of two experiments as in (D). The amount of *PGKC* mRNA in cells without an RNAi construct (WT) was set to 1.0; for *EP* and *PGKB*, the amount of mRNA at 48 h was set to 1.0. A third experiment gave similar results but the signals were too faint for quantitation.

Finally, results in Figure 4C had suggested that XRNA depletion stabilized an intermediate of about 400 nt. Since this fragment had not been detected from *CAT-EP* mRNAs after XRNA depletion (61), we suspected that it might depend on the *EP* coding region. We looked for such RNAs using primers 52 and 35; the latter hybridizes within the repetitive region encoding the EP repeats. The result was a clean ladder of products which was unaffected by either RNase H decapping or XRNA depletion (Figure 5C). All clones obtained, (with or without XRNA depletion) started at position +51 downstream of the ATG, and ended at position 10 in the 3′-UTR. This was paradoxical since no clones obtained with other primers had these boundaries.

Two novel findings emerged from this approach. First, we saw hitherto unsuspected heterogeneity in polyadenylation of *EP* mRNAs in bloodstream forms. Second, XRNA depletion caused accumulation of *EP* mRNA degradation intermediates that lacked not only the poly(A) tail, but also portions of the 5′-end. We were disappointed that we could not establish an upper poly(A) length threshold for deadenylation-dependent decapping; nevertheless, it was interesting that cloned *EP* mRNAs had much shorter poly(A)s than the *RPL37A* clones.

RNAi targeting a MEX67 homologue does not accelerate *EP* mRNA decay

XRNA is present in both the nucleus and the cytoplasm, so could theoretically attack *EP* and *PGKB* mRNA immediately after synthesis, prior to nuclear export. To address this possibility, we searched for homologues of the export factor MEX67 (human TAP). The protein predicted from one, Tb927.5.1270, is only 216 amino acids long, and RNAi had no effect on growth (data not shown). The protein encoded by Tb11.22.0004 is, in contrast, closer to the expected length, has two NTF2 homology domains (superfamily SSF54427), and is 30% identical (49% similar) to mouse TAP/MEX67 over the first 158 amino acids. RNAi targeting Tb11.22.0004 inhibited growth (Figure 8A). We used *in situ* hybridization to examine the distribution of poly(A) after RNAi targeting Tb11.22.0004. In normal cells, or RNAi cells without tetracycline addition, poly(A) was always distributed uniformly throughout the cytoplasm and nucleus (Figure 8B).

After RNAi, the cells showed a range of phenotypes, varying from normal poly(A) staining to strong retention of poly(A) in the nucleus (Figure 8C). These results, seen with several independent RNAi lines, suggest that the Tb11.22.0004 locus indeed encodes a MEX67-like protein that is required for mRNA export, so we have named the gene *TbMEX67*.

If the XRNA pathway were in the nucleus, one would expect a decrease in *EP* and *PGKB* mRNAs after *MEX67* RNAi. Instead, *MEX67* RNAi reproducibly caused an increase in both mRNAs (Figure 8D and E). At the same time, *PGKC* mRNA decreased. In normal bloodstream forms, the *PGKC:PGKB* ratio was greater than 10:1; after *MEX67* RNAi, the ratio changed to about 4:1. Results of a preliminary cell fractionation experiment suggested that even after 48 h tetracycline treatment, most of the *EP* mRNA was in the cytoplasm (data not shown). This is consistent with the *in situ* hybridization results suggesting that mRNA export from the nucleus had slowed down, but not stopped. These results lent no support to the notion that degradation of either *EP* or *PGKB* mRNA occurs in the nucleus.

DISCUSSION

Roles of PAN2 and PAN3 in trypanosomes

In yeast and animals, the roles of the PAN2/PAN3 complex may be mainly in quality control—trimming poly(A) tails in the nucleus and cytoplasm. The complex is not essential in yeast, and appears to have been lost many times in eukaryotic evolution. In addition, some organisms have truncated or mutant versions of PAN2 which have lost active site residues. PAN3 was present in most organisms that had PAN2, but absent in all that lacked it. Even in *Plasmodium*, which shows translational regulation (95) and has few potential regulatory transcription factors (96), we could find no PAN2/3.

Homologues of *PAN2* and *PAN3* are present in the trypanosome genome. Results from RNAi suggested that PAN2 is required for optimal trypanosome growth. We found no indication that PAN3 is required for PAN2 activity, and evidence for a PAN2–PAN3 interaction was weak. The effects of RNAi targeting *PAN2* were difficult to analyse since the RNAi effect was rapidly lost during culture. Nevertheless, it was clear that even when PAN2 depletion was sufficient to stop trypanosome growth, the degradation kinetics of several mRNAs were unchanged. In contrast, there was clear stabilization of the regulated *EP* mRNA and mild inhibition of *ACT* and *CAT-PGKB* mRNA decay. These results suggest that PAN2 may have a specialized role in degrading some, but not all mRNAs.

Decapping in trypanosomes

Decapping has been seen in trypanosome extracts (60), and was also measured indirectly in *Leishmania* (97). RNAi targeting the only reasonable candidate for a trypanosome DCP2-like decapping enzyme, Tb10.70.2530, did not affect cell growth (for details see Supplementary Data). We therefore wondered whether trypanosome mRNAs were decapped by some other mechanism. Since all mRNAs have a 5′ *SL*, sequence-specific endonuclease digestion within the *SL* could substitute for decapping. To analyse this we used RNA ligation and PCR to clone mRNA degradation intermediates. When we examined decay intermediates of the mRNA encoding ribosomal protein L37A, there was a favoured 5′-end, at positions 28–31 of the *SL*. However, the frequency of this was not increased after XRNA depletion, as would be expected for an endonuclease product. Moreover, some *L37A* RNAs had more *SL* sequence, and a similar pattern was not seen for *EP* mRNA. The result for *L37A* could be an artefact of the method. If it is not, there might be an *SL*-specific endonuclease, affecting some, but not all, mRNAs. Alternatively, XRNA (or another unidentified 5′–3′ exoribonuclease) may pause *in vivo* at position 28–31 because of secondary structure or the presence of bound protein.

CAF1 depletion increased the steady-state abundance of *EP* mRNA

Depletion of CAF1 almost completely stopped degradation of *HISH4*, *TUB*, *ACT* and *PGKC* mRNAs but the steady-state abundances were unaffected (14). We previously suggested that when mRNA degradation is stopped, a feedback mechanism might inhibit RNA polymerase II transcription. In contrast, depletion of CAF1 selectively increased the abundances of *EP* mRNA, which is made by RNA polymerase I. It is therefore possible that if a feedback mechanism exists, RNA polymerase I is less susceptible to it than RNA polymerase II. Also, it has recently been shown in *S. cerevisiae* that the Rpb4 and Rpb7 subunits of RNA polymerase II play roles in mRNA degradation (98,99). It is conceivable that these subunits also influence mRNA decay in trypanosomes (100).

Deadenylation and decapping of the *L37A* mRNA

In mammalian cells, decapping occurs on mRNAs that have reduced poly(A) tail lengths; the threshold may correspond to a minimum number of 25-nt-binding sites for PABP (101,102). In studies of budding yeast, the deadenylation limit is indeed 10–20 residues (103,104) though not many transcripts have been analysed in detail. A study of four mammalian liver mRNAs, using circularization, found that for one, decapped mRNAs had poly(A) tails of 20–60 nt, but the three others had shorter tails; there was no obvious relationship between the minimum tail length and the mRNA half-life (89). The stable beta-globin mRNA exhibits synchronous deadenylation until the poly(A) tail has a length of about 110 nt; after that, an asynchronous reduction to A(20) is observed before the mRNA is degraded (26). In contrast, completely deadenylated cmyc mRNA has been detected (105).

Our previous experiments had suggested that the poly(A) tails on histone H4 mRNA are reduced to about 50 nt before the mRNA body is degraded (14,61). Our attempts to analyse overall poly(A) lengths of the *L37A* mRNA by sequencing RT–PCR amplified, circularized mRNAs were thwarted by methodological bias towards shorter products. Nevertheless, the majority of

products were consistent with deadenylation-dependent decay. XRNA depletion had no effect on the overall pattern, and we can suggest a lower limit of $A_{(30–40)}$ for the threshold for decapping. The presence of short tails in nearly half of the decapped intermediates implies a temporal and mechanistic discontinuity in the decay process: after deadenylation reaches the threshold, the mRNA is decapped, but there is then a pause while the short-tailed, decapped mRNA is 'handed over' to the 5′–3′ exoribonuclease and/or the exosome.

Polyadenylation of *EP* mRNA

All evidence from northern blotting indicates that most *EP* mRNAs in bloodstream-form trypanosomes are polyadenylated at approximately the same position as in procyclic forms, about 300 nt downstream of the stop codon, and that the poly(A) tail is at least 50-nt long (see e.g. Figure 4). We were therefore surprised that after circle-PCR, almost all of the cloned polyadenylated *EP* RNAs had shorter 3′-UTRs. If such mRNAs were as abundant as the cloning results imply, the northern would have a smear and no full-length band at all. These mRNAs are nevertheless probably present, albeit at much lower abundance than the cloning results suggest. They could arise by use of alternative processing signals: this has been seen for *EP* before, but only in reporters with deletions of the wild-type sequence (87,106), Alternatively, oligo(A) tails might have been added to degradation intermediates in the cytoplasm. The exosome from some Archaea has the ability to add nucleotides to RNA; adenosine is added preferentially because ATP is most abundant in the cytoplasm (107). The trypanosome exosome lacks RNase PH activity (108), so is unlikely to be able to catalyse the polyadenylation reaction, but some other cytoplasmic protein might conceivably have this function.

Pathways of *EP* mRNA degradation

We previously suggested that in bloodstream-form trypanosomes, *CAT-EP*, *EP* and *PGKB* mRNAs are destroyed by two pathways, one dependent on XRNA and the other on deadenylation. The results presented here suggest a more complicated picture. The presence of very active, and at least partially deadenylation- independent, 5′–3′ pathway for *EP* mRNA degradation is supported by the presence of polyadenylated *CAT-GC-EP* degradation intermediates, and by the inhibition of degradation by depletion of XRNA. However, we also found deadenylated *CAT-GC-EP* intermediates, and 3′–5′ exonuclease products from both *CAT-GC-EP* and *EP*. The *EP* mRNA degradation kinetics included a fast, XRNA-dependent component and a slower one dependent on CAF1. Even the rapid degradation pathway, had a 3′-exonucleolytic component: it was made slower by CAF1 depletion, and was delayed by RNAi targeting the exosome (74).

Yeast XRN1 is processive on a poly(A) substrate (109). If XRNA were processive on mRNA *in vivo*, a reduction in the XRNA level should cause accumulation of full-length, but decapped *EP* mRNA, but should not change the overall distribution of mRNAs in which are 'caught in the act' of 5′ degradation at the time of RNA isolation. If XRNA were distributive *in vivo*, RNAi should cause accumulation of many different 5′ degradation products; the same picture would be obtained if, after XRNA depletion, decapped mRNAs were degraded by a different, distributive, 5′–3′ exoribonuclease. Inhibition by secondary structures, bound proteins and ribosomes could also affect the pattern. We found that the cloned intermediates from XRNA-depleted cells were significantly shorter at the 5′-end than those from normal cells. There are multiple possible explanations, and we present just one, highly speculative, scenario here. Suppose that in normal cells, XRNA is responsible for most 5′–3′ degradation: its activity is transiently delayed by the exon junction complex or other proteins bound to the spliced leader; but once over this barrier, digestion is processive. This would explain the predominance of intermediates that retain parts of the spliced leader in normal cells. In the absence of XRNA, decapped mRNA accumulates, and is either attacked from the 3′-end, or degraded from the 5′-end by other, distributive exoribonucleases, or by endonucleases.

When CAF1 was depleted, half of the *EP* mRNA was degraded within 15 min, but the rest appeared to be very stable, and so apparently not susceptible to degradation by other enzymes. This suggests mechanistic separation of the CAF1-dependent and -independent pathways. Temporal separation, with deadenylation-independent degradation only within the first 15 min after synthesis, would be easily understood if the XRNA pathway were located in the nucleus; but this is unlikely, since *EP* mRNA accumulated after depletion of MEX67. *CAF1* RNAi might also result in abnormal sequestering of mRNAs in stress granules (62) or other structures (110). We looked for this, but 24 h after induction of RNAi against either *CAF1* or *NOT1* there was little, if any effect on the distribution of the helicase DHH1 (data not shown), which is a stress granule marker (62).

We suggest that the choice of mRNA degradation pathway is dictated by binding of different combinations of regulatory RNA-binding proteins. The *RPL37A*, *HISH4* and other relatively stable mRNAs are bound by combinations of RNA-binding proteins that actively prevent degradation (111); deadenylation is slow, but at a threshold (minimally, $A_{30–40}$) there is a pause before subsequent attack at the 5′ and 3′ ends. Protein combinations specific for *EP*, *PGKB* and related unstable mRNAs, in contrast, can actively recruit either XRNA and the elusive decapping enzyme, or deadenylases; this causes either very rapid degradation initiated from the 5′-end, or a rapid entry to the deadenylation-dependent pathway. If XRNA is not available, the mRNA defaults to the deadenylation-dependent pathway. Possibly, the RNA-binding proteins route the highly unstable mRNAs directly to P-bodies.

This scenario is entirely consistent with results from other eukaryotes. For example, the alpha1 tubulin mRNA of *Chlamydomonas reinhardtii* is normally degraded via deadenylation followed by decapping and 5′–3′ digestion. After deflagellation, synthesis of the mRNAs is induced, but their half-lives decrease to 10–15 min, and 5′ degradation occurs without deadenylation (112). Mammalian mRNAs with different AU-rich

elements also show different deadenylation kinetics (113). The next challenge, for trypanosomes, consists in identifying the RNA-binding proteins that guide these choices.

SUPPLEMENTARY DATA

Supplementary Data are available at NAR Online.

ACKNOWLEDGEMENTS

The authors thank Prof. Luise Krauth-Siegel (BZH, Heidelberg) for providing antibody to trypanothione reductase, and Mark Carrington and Louise Ellis (University of Cambridge, England) for information about the PAN2 open reading frame. This work was supported by the Deutsche Forschungsgemeinschaft. They also thank Diana Inchaustegui for doing some of the circle PCR experiments and Stuart Archer for checking the manuscript.

FUNDING

EMBO short-term fellowship to N.B. Funding for open access charge: State of Baden-Württemburg.

Conflict of interest statement. None declared.

REFERENCES

1. Caponigro,G. and Parker,R. (1995) Multiple functions for the poly(A)-binding protein in mRNA decapping and deadenylation in yeast. *Genes Dev.*, **9**, 2421–2432.
2. Tharun,S. and Parker,R. (2001) Targeting an mRNA for decapping: displacement of translation factors and association of the Lsm1p-7p complex on deadenylated yeast mRNAs. *Mol. Cell*, **8**, 1075–1083.
3. Wilusz,C.J., Gao,M., Jones,C.L., Wilusz,J. and Peltz,S.W. (2001) Poly(A)-binding proteins regulate both mRNA deadenylation and decapping in yeast cytoplasmic extracts. *RNA*, **7**, 1416–1424.
4. Körner,C.G., Wormington,M., Muckenthaler,M., Schneider,S., Dehlin,E. and Wahle,E. (1998) The deadenylating nuclease (DAN) is involved in poly(A) tail removal during the meiotic maturation of Xenopus oocytes. *EMBO J.*, **17**, 5427–5437.
5. Dehlin,E., Wormington,M., Körner,C.G. and Wahle,E. (2000) Cap-dependent deadenylation of mRNA. *EMBO J.*, **19**, 1079–1086.
6. Reverdatto,S.V., Dutko,J.A., Chekanova,J.A., Hamilton,D.A. and Belostotsky,D.A. (2004) mRNA deadenylation by PARN is essential for embryogenesis in higher plants. *RNA*, **10**, 1200–1214.
7. Körner,C.G. and Wahle,E. (1997) Poly(A) tail shortening by a mammalian poly(A)-specific 3′-exoribonuclease. *J. Biol. Chem.*, **272**, 10448–10456.
8. Temme,C., Zaessinger,S., Meyer,S., Simonelig,M. and Wahle,E. (2004) A complex containing the CCR4 and CAF1 proteins is involved in mRNA deadenylation in Drosophila. *EMBO J.*, **23**, 2862–2871.
9. Collart,M. and Timmers,H. (2004) The eukaryotic Ccr4-Not complex: A regulatory platform Integrating mRNA metabolism with cellular signaling pathways? *Prog. Nucleic Acid Res. Mol. Biol.*, **77**, 289.
10. Albert,T.K., Lemaire,M., van Berkum,N.L., Gentz,R., Collart,M.A. and Timmers,H.T. (2000) Isolation and characterization of human orthologs of yeast CCR4-NOT complex subunits. *Nucleic Acids Res.*, **28**, 809–817.
11. Chen,J., Rappsilber,J., Chiang,Y.C., Russell,P., Mann,M. and Denis,C.L. (2001) Purification and characterization of the 1.0 MDa CCR4-NOT complex identifies two novel components of the complex. *J. Mol. Biol.*, **314**, 683–694.
12. Tucker,M., Valencia-Sanchez,M.A., Staples,R.R., Chen,J., Denis,C.L. and Parker,R. (2001) The transcription factor associated Ccr4 and Caf1 proteins are components of the major cytoplasmic mRNA deadenylase in *Saccharomyces cerevisiae*. *Cell*, **104**, 377–386.
13. Tucker,M., Staples,R.R., Valencis-Sanchez,M.A., Muhlrad,D. and Parker,R. (2002) Ccr4p is the catalytic subunit of a Ccr4p/Pop2p/Notp mRNA deadenylase complex in *Saccharomyces cerevisiae*. *EMBO J.*, **21**, 1427–1436.
14. Schwede,A., Ellis,L., Luther,J., Carrington,M., Stoecklin,G. and Clayton,C. (2008) An essential role for Caf1 in mRNA deadenylation in trypanosomes and human cells. *Nucleic Acids Res.*, **36**, 3374–3388.
15. Zheng,D., Ezzeddine,N., Chen,C.-Y., Zhu,W., He,X. and Shyu,A.-B. (2008) Deadenylation is prerequisite for P-body formation and mRNA decay in mammalian cells. *J. Cell Biol.*, **182**, 89–101.
16. Molin,L. and Puisieux,A. (2005) *C. elegans* homologue of the Caf1 gene, which encodes a subunit of the CCR4-NOT complex, is essential for embryonic and larval development and for meiotic progression. *Gene*, **358**, 73–81.
17. Gao,M., Fritz,D.T., Ford,L.P. and Wilusz,J. (2000) Interaction between a poly(A) specific ribonuclease and the 5′ cap influences mRNA deadenylation rates in vitro. *Mol. Cell*, **5**, 479–488.
18. Daugeron,M.C., Mauxion,F. and Seraphin,B. (2001) The yeast POP2 gene encodes a nuclease involved in mRNA deadenylation. *Nucleic Acids Res.*, **29**, 2448–2455.
19. Lowell,J.E., Rudner,D.Z. and Sachs,A.B. (1992) 3′-UTR-dependent deadenylation by the yeast poly(A) nuclease. *Genes Dev.*, **6**, 2088–2099.
20. Uchida,N., Hoshino,S. and Katada,T. (2004) Identification of a human cytoplasmic poly(A) nuclease complex stimulated by poly(A)-binding protein. *J. Biol. Chem.*, **279**, 1383–1391.
21. Siddiqui,N., Mangus,D.A., Chang,T.C., Palermino,J.M., Shyu,A.B. and Gehring,K. (2007) Poly(A) nuclease interacts with the C-terminal domain of polyadenylate-binding protein domain from poly(A)-binding protein. *J. Biol. Chem.*, **282**, 25067–25075.
22. Brown,C.E. and Sachs,A.B. (1998) Poly(A) tail length control in Saccharomyces cerevisiae occurs by message-specific deadenylation. *Mol. Cell Biol.*, **18**, 6548–6559.
23. Boeck,R., Tarun,S. Jr, Rieger,M., Deardorff,J.A., Muller-Auer,S. and Sachs,A.B. (1996) The yeast Pan2 protein is required for poly(A)-binding protein-stimulated poly(A)-nuclease activity. *J. Biol. Chem.*, **271**, 432–438.
24. Brown,C.E., Tarun,S.Z. Jr, Boeck,R. and Sachs,A.B. (1996) PAN3 encodes a subunit of the Pab1p-dependent poly(A) nuclease in Saccharomyces cerevisiae. *Mol. Cell Biol.*, **16**, 5744–5753.
25. Bönisch,C., Temme,C., Moritz,B. and Wahle,E. (2007) Degradation of *HSP70* and other mRNAs in *Drosophila* via the 5′-3′ pathway and its regulation by heat shock. *J. Biol. Chem.*, **282**, 21818–21828.
26. Yamashita,A., Chang,T.C., Yamashita,Y., Zhu,W., Zhong,Z., Chen,C.Y. and Shyu,A.B. (2005) Concerted action of poly(A) nucleases and decapping enzyme in mammalian mRNA turnover. *Nat. Struct. Mol. Biol.*, **12**, 1054–1063.
27. Decker,C.J. and Parker,R. (1993) A turnover pathway for both stable and unstable mRNAs in yeast: evidence for a requirement for deadenylation. *Genes Dev.*, **7**, 1632–1643.
28. Muhlrad,D., Decker,C.J. and Parker,R. (1994) Deadenylation of the unstable mRNA encoded by the yeast MFA2 gene leads to decapping followed by 5′-3′ digestion of the transcript. *Genes Dev.*, **8**, 855–866.
29. Muhlrad,D., Decker,C.J. and Parker,R. (1995) Turnover mechanisms of the stable yeast PGK1 mRNA. *Mol. Cell Biol.*, **15**, 2145–2156.
30. Anderson,J. and Parker,R. (1998) The 3′ to 5′ degradation of yeast mRNAs is a general mechanism for mRNA turnover that requires the SKI2 DEVH box protein and 3′ to 5′ exonucleases of the exosome complex. *EMBO J.*, **17**, 1497–1506.
31. Jacobs Anderson,J.S. and Parker,R.P. (1998) The 3′ to 5′ degradation of yeast mRNAs is a general mechanism for mRNA turnover that requires the SKI2 DEVH box protein and 3′ to 5′ exonucleases of the exosome complex. *EMBO J.*, **17**, 1497–1506.
32. Wang,Z. and Kiledjian,M. (2001) Functional link between the mammalian exosome and mRNA decapping. *Cell*, **107**, 751–762.

33. Cao,D. and Parker,R. (2001) Computational modeling of eukaryotic mRNA turnover. *RNA*, **7**, 1192–1212.
34. Chen,C.Y., Xu,N. and Shyu,A.B. (1995) mRNA decay mediated by two distinct AU-rich elements from c-fos and granulocyte-macrophage colony-stimulating factor transcripts: different deadenylation kinetics and uncoupling from translation. *Mol. Cell Biol.*, **15**, 5777–5788.
35. Lai,W.S., Carballo,E., Strum,J.R., Kennington,E.A., Phillips,R.S. and Blackshear,P.J. (1999) Evidence that tristetraprolin binds to AU-rich elements and promotes the deadenylation and destabilization of tumor necrosis factor alpha mRNA. *Mol. Cell Biol.*, **19**, 4311–4323.
36. Xu,N., Loflin,P., Chen,C.Y. and Shyu,A.B. (1998) A broader role for AU-rich element-mediated mRNA turnover revealed by a new transcriptional pulse strategy. *Nucleic Acids Res.*, **26**, 558–565.
37. Stoecklin,G., Mayo,T. and Anderson,P. (2006) ARE-mRNA degradation requires the 5′–3′ decay pathway. *EMBO Rep.*, **7**, 72–77.
38. Murray,E.L. and Schoenberg,D.R. (2007) A + U-rich instability elements differentially activate 5′-3′ and 3′-5′ mRNA decay. *Mol. Cell Biol.*, **27**.
39. Rodgers,N., Wang,Z. and Kiledjian,M. (2002) Regulated alpha-globin mRNA decay is a cytoplasmic event proceeding through 3′-to-5′ exosome-dependent decapping. *RNA*, **8**, 1526–1537.
40. Chen,C.Y. and Shyu,A.B. (2003) Rapid deadenylation triggered by a nonsense codon precedes decay of the RNA body in a mammalian cytoplasmic nonsense-mediated decay pathway. *Mol. Cell Biol.*, **23**, 4805–4813.
41. Mitchell,P. and Tollervey,D. (2003) An NMD pathway in yeast involving accelerated deadenylation and exosome-mediated 3′—>5′ degradation. *Mol. Cell*, **11**, 1405–1413.
42. Takahashi,S., Araki,Y., Sakuno,T. and Katada,T. (2003) Interaction between Ski7p and Upf1p is required for nonsense-mediated 3′-to-5′ mRNA decay in yeast. *EMBO J*, **22**, 3951–3959.
43. Pantopoulos,K. (2004) Iron metabolism and the IRE/IRP regulatory system: an update. *Ann. NY Acad. Sci.*, **1012**, 1–13.
44. Wang,Z. and Kiledjian,M. (2000) The poly(A) binding protein and an mRNA stability protein jointly regulate an endoribonuclease activity. *Mol. Cell Biol.*, **20**, 6334–6341.
45. Yang,F. and Schoenberg,D. (2004) Endonuclease-mediated mRNA decay involves the selective targeting of PMR1 to polyribosome-bound substrate mRNA. *Mol. Cell*, **14**, 435–445.
46. Gatfield,D. and Izaurralde,E. (2004) Nonsense-mediated messenger RNA decay is initiated by endonucleolytic cleavage in *Drosophila*. *Nature*, **429**, 575–578.
47. Huntzinger,E., Kashima,I., Fauser,M., Saulière,J. and Izaurralde,E. (2008) SMG6 is the catalytic endonuclease that cleaves mRNAs containing nonsense codons in metazoan. *RNA*, **14**, 2609–2617.
48. Eberle,A., Lykke-Andersen,S., Mühlemann,O. and Jensen,T. (2008) SMG6 promotes endonucleolytic cleavage of nonsense mRNA in human cells. *Nat. Struct. Mol. Biol.*, **16**, 49–55.
49. Hatfield,L., Beelman,C.A., Stevens,A. and Parker,R. (1996) Mutations in trans-acting factors affecting mRNA decapping in *Saccharomyces cerevisiae*. *Mol. Cell Biol.*, **16**, 5830–5838.
50. Badis,G., Saveanu,C., Fromont-Racine,M. and Jacquier,A. (2004) Targeted mRNA degradation by deadenylation-independent decapping. *Mol. Cell*, **15**, 5–15.
51. Muhlrad,D. and Parker,R. (2005) The yeast EDC1 mRNA undergoes deadenylation-independent decapping stimulated by Not2p, Not4p, and Not5p. *EMBO J.*, **24**, 1033–1045.
52. van Hoof,A., Frischmeyer,P.A., Dietz,H.C. and Parker,R. (2002) Exosome-mediated recognition and degradation of mRNAs lacking a termination codon. *Science*, **295**, 2262–2264.
53. Mullen,T.E. and Marzluff,W.F. (2008) Degradation of histone mRNA requires oligouridylation followed by decapping and simultaneous degradation of the mRNA both 5′ to 3′ and 3′ to 5′. *Genes Dev.*, **22**, 50–65.
54. Rodrıguez-Ezpeleta,N., Brinkmann,H., Burger,G., Roger,A., Gray,M., Philippe,H. and Lang,B. (2007) Toward resolving the eukaryotic tree: the phylogenetic positions of Jakobids and Cercozoans. *Curr. Biol.*, **17**, 1420–1425.
55. Martinez-Calvillo,S., Yan,S., Nguyen,D., Fox,M., Stuart,K. and Myler,P.J. (2003) Transcription of Leishmania major Friedlin chromosome 1 initiates in both directions within a single region. *Mol. Cell*, **11**, 1291–1299.
56. Gibson,W.C., Swinkels,B.W. and Borst,P. (1988) Post-transcriptional control of the differential expression of phosphoglycerate kinase genes in *Trypanosoma brucei*. *J. Mol. Biol.*, **201**, 315–325.
57. Liang,X., Haritan,A., Uliel,S. and Michaeli,S. (2003) *Trans* and *cis* splicing in trypanosomatids: mechanism, factors, and regulation. *Eukaryot. Cell*, **2**, 830–840.
58. Brems,S., Guilbride,D.L., Gundlesdodjir-Planck,D., Busold,C., Luu,V.D., Schanne,M., Hoheisel,J. and Clayton,C. (2005) The transcriptomes of *Trypanosoma brucei* Lister 427 and TREU927 bloodstream and procyclic trypomastigotes. *Mol. Biochem. Parasitol.*, **139**, 163–172.
59. Clayton,C. and Shapira,M. (2007) Post-transcriptional regulation of gene expression in trypanosomes and leishmanias. *Mol. Biochem. Parasitol.*, **156**, 93–101.
60. Milone,J., Wilusz,J. and Bellofatto,V. (2002) Identification of mRNA decapping activities and an ARE-regulated 3′ to 5′ exonuclease activity in trypanosome extracts. *Nucleic Acids Res.*, **30**, 4040–4050.
61. Li,C.-H., Irmer,H., Gudjonsdottir-Planck,D., Freese,S., Salm,H., Haile,S., Estévez,A.M. and Clayton,C.E. (2006) Roles of a *Trypanosoma brucei* 5′->3′ exoribonuclease homologue in mRNA degradation. *RNA*, **12**, 2171–2186.
62. Kramer,S., Queiroz,R., Ellis,L., Webb,H., Hoheisel,J., Clayton,C. and Carrington,M. (2008) Heat shock causes a decrease in polysomes and the appearance of stress granules in trypanosomes independently of eIF2 phosphorylation at Thr169. *J. Cell Sci.*, **121**, 3002–3014.
63. Gunzl,A., Bruderer,T., Laufer,G., Schimanski,B., Tu,L.C., Chung,H.M., Lee,P.T. and Lee,M.G. (2003) RNA polymerase I transcribes procyclin genes and variant surface glycoprotein gene expression sites in *Trypanosoma brucei*. *Eukaryot. Cell*, **2**, 542–551.
64. Biebinger,S., Rettenmaier,S., Flaspohler,J., Hartmann,C., Peña-Diaz,J., Wirtz,L.E., Hotz,H.R., Barry,J.D. and Clayton,C.E. (1996) The PARP promoter of *Trypanosoma brucei* is developmentally regulated in a chromosomal context. *Nucleic Acids Res.*, **24**, 1202–1211.
65. Hotz,H.-R., Biebinger,S., Flaspohler,J. and Clayton,C.E. (1998) *PARP* gene expression: regulation at many levels. *Mol. Biochem. Parasitol.*, **91**, 131–143.
66. Engstler,M. and Boshart,M. (2004) Cold shock and regulation of surface protein trafficking convey sensitization to inducers of stage differentiation in *Trypanosoma brucei*. *Genes Dev.*, **18**, 2798–2811.
67. Haanstra,J., Stewart,M., Luu,V.-D., van Tuijl,A., Westerhoff,H., Clayton,C. and Bakker,B. (2008) Control and regulation of gene expression: quantitative analysis of the expression of phosphoglycerate kinase in bloodstream form *Trypanosoma brucei*. *J. Biol. Chem.*, **283**, 2495–2507.
68. Irmer,H. and Clayton,C.E. (2001) Degradation of the *EP1* mRNA in *Trypanosoma brucei* is initiated by destruction of the 3′-untranslated region. *Nucleic Acids Res.*, **29**, 4707–4715.
69. Hotz,H.-R., Hartmann,C., Huober,K., Hug,M. and Clayton,C.E. (1997) Mechanisms of developmental regulation in *Trypanosoma brucei*: a polypyrimidine tract in the 3′-untranslated region of a trypanosome surface protein mRNA affects RNA abundance and translation. *Nucleic Acids Res.*, **25**, 3017–3025.
70. Quijada,L., Hartmann,C., Guerra-Giraldez,C., Drozdz,M., Irmer,H. and Clayton,C.E. (2002) Expression of the human RNA-binding protein HuR in *Trypanosoma brucei* induces differentiation-related changes in the abundance of developmentally-regulated mRNAs. *Nucleic Acids Res.*, **30**, 1–11.
71. Schürch,N., Furger,A., Kurath,U. and Roditi,I. (1997) Contribution of the procyclin 3′ untranslated region and coding region to the regulation of expression in bloodstream forms of *Trypanosoma brucei*. *Mol. Biochem. Parasit.*, **89**, 109–121.
72. Furger,A., Schürch,N., Kurath,U. and Roditi,I. (1997) Elements in the 3′ untranslated region of procyclin mRNA regulate expression in insect forms of *Trypanosoma brucei* by modulating RNA stability and translation. *Mol. Cell Biol.*, **17**, 4372–4380.
73. Drozdz,M. and Clayton,C.E. (1999) Structure of a regulatory 3′-untranslated region from *Trypanosoma brucei*. *RNA*, **5**, 1632–1644.

74. Haile,S., Estévez,A.M. and Clayton,C. (2003) A role for the exosome in the initiation of degradation of unstable mRNAs. *RNA*, **9**, 1491–1501.
75. Alibu,V.P., Storm,L., Haile,S., Clayton,C. and Horn,D. (2004) A doubly inducible system for RNA interference and rapid RNAi plasmid construction in *Trypanosoma brucei*. *Mol. Biochem. Parasitol.*, **139**, 75–82.
76. Shi,H., Djikeng,A., Mark,T., Wirtz,E., Tschudi,C. and Ullu,E. (2000) Genetic interference in *Trypanosoma brucei* by heritable and inducible double-stranded RNA. *RNA*, **6**, 1069–1076.
77. Clayton,C.E., Estévez,A.M., Hartmann,C., Alibu,V.P., Field,M. and Horn,D. (2005) In Carmichael,G. (ed.), *RNA interference*. Humana Press, Totowa, New Jersey, USA.
78. Shen,S., Arhin,G.K., Ullu,E. and Tschudi,C. (2001) In vivo epitope tagging of *Trypanosoma brucei* genes using a one step PCR-based strategy. *Mol. Biochem. Parasitol.*, **113**, 171–173.
79. Colasante,C., Alibu,V.P., Kirchberger,S., Tjaden,J., Clayton,C. and Voncken,F. (2006) Characterisation and developmentally regulated localisation of the mitochondrial carrier protein homologue MCP6 from *Trypanosoma brucei*. *Eukaryot Cell*, **5**, 1194–1205.
80. Colasante,C., Robles,A., Li,C.-H., Schwede,A., Benz,C., Voncken,F., Guilbride,D.L. and Clayton,C. (2007) Regulated expression of glycosomal phosphoglycerate kinase in *Trypanosoma brucei*. *Mol. Biochem. Parasitol.*, **151**, 193–204.
81. Kirkwood,B. and Stern,J. (2003) *Essential Medical Statistics*. Blackwood, Oxford.
82. Cassola,A., De Gaudenzi,J. and Frasch,A. (2007) Recruitment of mRNAs to cytoplasmic ribonucleoprotein granules in trypanosomes. *Mol. Microbiol.*, **65**, 655–670.
83. Zeiner,G.M., Sturm,N.R. and Campbell,D.A. (2003) Exportin 1 mediates nuclear export of the Kinetoplastid spliced leader RNA. *Eucaryot. Cell*, **2**, 222–230.
84. Marchler-Bauer,A., Anderson,J., Derbyshire,M., DeWeese-Scott,C., Gonzales,N., Gwadz,M., Hao,L., He,S., Hurwitz,D., Jackson,J. *et al.* (2007) CDD: a conserved domain database for interactive domain family analysis. *Nucleic Acids Res.*, **35**, D237–D240.
85. Hu,M., Li,P., Li,M., Li,W., Yao,T., Wu,J.-W., Gu,W., Cohen,R. and Shi,Y. (2002) Crystal Structure of a UBP-family deubiquitinating enzyme in isolation and in complex with ubiquitin aldehyde. *Cell*, **111**, 1041–1054.
86. Pays,E., Coquelet,H., Tebabi,P., Pays,A., Jefferies,D., Steinert,M., Koenig,E., Williams,R.O. and Roditi,I. (1990) *Trypanosoma brucei*: constitutive activity of the VSG and procyclin gene promoters. *EMBO J.*, **9**, 3145–3151.
87. Hug,M., Hotz,H.R., Hartmann,C. and Clayton,C.E. (1994) Hierarchies of RNA processing signals in a trypanosome surface antigen mRNA precursor. *Mol. Cell Biol.*, **14**, 7428–7435.
88. Lackner,D., Beilharz,T., Marguerat,S., Mata,J., Watt,S., Schubert,F., Preiss,T. and Bähler,J. (2007) A network of multiple regulatory layers shapes gene expression in fission yeast. *Mol. Cell*, **26**, 145–155.
89. Couttet,P., Fromont-Racine,M., Steel,D., Pictet,R. and Grange,T. (1997) Messenger RNA deadenylation precedes decapping in mammalian cells. *Proc. Natl Acad. Sci. USA*, **94**, 5628–5633.
90. Freistadt,M., Cross,G. and Robertson,H. (1988) Discontinuously synthesized mRNA from *Trypanosoma brucei* contains the highly methylated 5′ cap structure, m7GpppA*A*C(2'-O)mU*A. *J. Biol. Chem.*, **263**, 15071–15075.
91. Freistadt,M., Cross,G., Branch,A. and Robertson,H. (1987) Direct analysis of the mini-exon donor RNA of *Trypanosoma brucei*: detection of a novel cap structure also present in messenger RNA. *Nucleic Acids Res.*, **15**, 9861–9879.
92. Perry,K.L., Watkins,K.P. and Agabian,N. (1987) Trypanosome mRNAs have unusual "cap 4" structures acquired by addition of a spliced leader. *Proc. Natl Acad. Sci. USA*, **84**, 8190–8194.
93. McNally,K.P. and Agabian,N. (1992) Trypanosoma brucei spliced-leader RNA methylations are required for trans splicing in vivo. *Mol. Cell Biol.*, **12**, 4844–4851.
94. Ullu,E. and Tschudi,C. (1991) Trans splicing in trypanosomes requires methylation of the 5′ end of the spliced leader RNA. *Proc. Natl Acad. Sci. USA*, **88**, 10074–10078.
95. Mair,G., Braks,J., Garver,L., Wiegant,J., Hall,N., Dirks,R., Khan,S., Dimopoulos,G., Janse,C. and Waters,A. (2006) Regulation of sexual development of *Plasmodium* by translational repression. *Science*, **313**, 667–669.
96. Iyer,L., Anantharaman,V., Wolf,M. and Aravind,L. (2008) Comparative genomics of transcription factors and chromatin proteins in parasitic protists and other eukaryotes. *Int. J. Parasitol.*, **38**, 1–31.
97. Haile,S., Dupe,A. and Papadopoulou,B. (2008) Deadenylation-independent stage-specific mRNA degradation in *Leishmania*. *Nucleic Acids Res.*, **36**, 1634–1644.
98. Lotan,R., Bar-On,V., Harel-Sharvit,L., Duek,L., Melamed,D. and Choder,M. (2005) The RNA polymerase II subunit Rpb4p mediates decay of a specific class of mRNAs. *Genes Dev.*, **19**, 3004–3016.
99. Lotan,R., Goler-Baron,V., Duek,L., Haimovich,G. and Choder,M. (2007) The Rpb7p subunit of yeast RNA polymerase II plays roles in the two major cytoplasmic mRNA decay mechanisms. *J. Cell Biol.*, **178**, 1133–1143.
100. Das,A., Li,H., Liu,T. and Bellofatto,V. (2006) Biochemical characterization of Trypanosoma brucei RNA polymerase II. *Mol. Biochem. Parasitol.*, **150**, 201–210.
101. Deo,R., Bonanno,J., Sonenberg,N. and Burley,S. (1999) Recognition of polyadenylate RNA by the poly(A)-binding protein. *Cell*, **98**, 835–845.
102. Baer,B. and Kornberg,R. (1983) The protein responsible for the repeating structure of cytoplasmic poly(A)-ribonucleoprotein. *J. Cell Biol.*, **96**, 717–721.
103. Simón,E. and Séraphin,B. (2007) A specific role for the C-terminal region of the Poly(A)-binding protein in mRNA decay. *Nucleic Acids Res.*, **35**, 6017–6028.
104. Prieto,S., de la Cruz,B. and Scheffler,I. (2000) Glucose-regulated turnover of mRNA and the influence of poly(A) tail length on half-life. *J. Biol. Chem.*, **275**, 14155–14166.
105. Brewer,G. (1999) Evidence for a 3′-5′ decay pathway for c-myc mRNA in mammalian cells. *J. Biol. Chem.*, **274**, 16174–16179.
106. Schürch,N., Hehl,A., Vassella,E., Braun,R. and Roditi,I. (1994) Accurate polyadenylation of procyclin mRNAs in *Trypanosoma brucei* is determined by pyrimidine-rich elements in the intergenic regions. *Mol. Cell Biol.*, **14**, 3668–3675.
107. Portnoy,V. and Schuster,G. (2006) RNA polyadenylation and degradation in different Archaea; roles of the exosome and RNase R. *Nucelic Acids Res.*, **34**, 5923–5931.
108. Cristodero,M., Böttcher,B., Diepholz,M., Scheffzeck,K. and Clayton,C. (2008) The exosome of *Leishmania tarentolae*: purification and structural analysis by electron microscopy. *Mol. Biochem. Parasitol.*, **159**, 24–29.
109. Stevens,A. (1980) Purification and characterization of a *Saccharomyces cerevisiae* exoribonuclease which yields 5′-mononucleotides by a 5′ leads to 3′ mode of hydrolysis. *J. Biol. Chem.*, **255**, 3080–3085.
110. Biton,M., Mandelboim,M., Arvatz,G. and Michaeli,S. (2006) RNAi interference of XPO1 and Sm genes and their effect on the spliced leader RNA in *Trypanosoma brucei*. *Mol. Biochem. Parasitol.*, **150**, 132–143.
111. Estévez,A. (2008) The RNA-binding protein *Tb*DRBD3 regulates the stability of a specific subset of mRNAs in trypanosomes. *Nucleic Acids Res.*, **36**, 4573–4586.
112. Gera,J.F. and Baker,E.J. (1998) Deadenylation-dependent and -independent decay pathways for a 1-tubulin mRNA in *Chlamydomonas reinhardtii*. *Mol. Cell Biol.*, **18**, 1498–1505.
113. Xu,N., Chen,C.Y. and Shyu,A.B. (1997) Modulation of the fate of cytoplasmic mRNA by AU-rich elements: key sequence features controlling mRNA deadenylation and decay. *Mol. Cell Biol.*, **17**, 4611–4621.
114. Cheng,Y. and Patel,D. (2004) Crystallographic structure of the nuclease domain of 3′hExo, a DEDDh family member, bound to rAMP. *J. Mol. Biol.*, **343**, 305–312.
115. de Silva,U., Choudhury,S., Bailey,S., Harvey,S., Perrino,F. and Hollis,T. (2007) The crystal structure of TREX1 explains the 3′ nucleotide specificity and reveals a polyproline II helix for protein partnering. *J. Biol. Chem.*, **282**, 10537–10543.